

Chapter 5

Summary of Quaternary Faulting on the Paintbrush Canyon, Bow Ridge, and Stagecoach Road Faults

By Christopher M. Menges, Emily M. Taylor, John R. Wesling,¹ Frank H. Swan,¹ Jeffrey A. Coe, Daniel J. Ponti, and John W. Whitney

Contents

Abstract.....	41
Introduction.....	42
Paintbrush Canyon Fault.....	42
Busted Butte.....	42
Trench MWV-T4.....	55
Trench A1.....	56
Bow Ridge Fault.....	58
Trench T14D.....	59
Trench T14.....	63
Stagecoach Road Fault.....	63
Trenches SCR-T1 and SCR-T3.....	63

Abstract

The Paintbrush Canyon, Bow Ridge, and Stagecoach Road Faults east and southeast of Yucca Mountain all show evidence of multiple Quaternary faulting events. Variations in available numerical-age control, in combination with uncertainties in both estimated age and (or) displacements, typically result in a range of such time-dependent faulting parameters as recurrence intervals and slip rates.

Gullies incised into sand ramps along the west side of Busted Butte expose the most complete record of Quaternary activity along the southern section of the Paintbrush Canyon Fault. Six to seven faulting events have been distinguished, with a cumulative dip-slip displacement of about 600 cm and preferred estimates of the net displacement per event ranging from 28 to 167 cm. Average preferred recurrence intervals range from 50 to 120 k.y., and for the three latest faulting events from 65 to 95 k.y. Preferred estimates of late Quater-

nary slip rates at Busted Butte range from 0.004 to 0.009 mm/yr, and long-term average slip rates for the entire post-early Pleistocene paleoseismic record in the Busted Butte exposures range from 0.008 to 0.01 mm/yr.

Trenches also reveal details of Quaternary fault activity. Trench MWV-T4, located on the central section of the Paintbrush Canyon Fault near the south end of Midway Valley, exposes a record of three or four Quaternary faulting events with an estimated cumulative dip-slip displacement of 170 to 270 cm and preferred estimates of the displacement per event of 20 to 98 cm. Average recurrence intervals range from 20 to 50 k.y., and slip rates from 0.01 to 0.03 mm/yr. Trench A1, which was excavated across the projected trace of the northern section of the Paintbrush Canyon Fault, exposes a 5-m-thick sequence of Quaternary deposits that shows evidence of at least four faulting events. Cumulative vertical displacement of Quaternary deposits is 145 to 170 cm, with calculated recurrence intervals of 80–100 k.y. and an estimated fault slip rate of 0.002 mm/yr.

The history of Quaternary activity on the Bow Ridge Fault is based largely on exposures in trench T14D, which was excavated across the northern section of the fault on the west side of Exile Hill. A well-defined sequence of alluvial, colluvial, and eolian deposits displays evidence of two or three middle to late Pleistocene faulting events, with preferred estimates of the net displacement per event ranging from 13 to 44 cm. Preferred average estimates of the recurrence interval and slip rate are 100–140 k.y. and 0.003 mm/yr, respectively. Trench T14, located about 50 m north of trench T14D, exposes a well-defined fault zone between Tertiary bedrock and Quaternary deposits that contains numerous vertical veins of secondary calcite and opaline silica whose origin is interpreted to be associated with downward percolation of meteoric water rather than with ascending spring water.

Fault relations on the Stagecoach Road Fault are well expressed in a 3- to 3.5-m-thick sequence of varied mid-Quaternary to upper Quaternary deposits that is exposed in

¹Geomatrix Consultants, Inc., Oakland, Calif.

trenches SCR-T1 and SCR-T3. Two to four late Pleistocene to Holocene(?) faulting events are represented, with a cumulative net displacement of 1.0 to 3.1 m and preferred estimates of the net and dip-slip displacements per event of 40 to 67 cm. The most internally consistent set of geochronologic controls, which also agrees with age correlations of disseminated basaltic-ash horizons, yields preferred estimates of the average paleoearthquake-recurrence intervals and fault-slip rate of 20–50 k.y. and 0.02 to 0.03 mm/yr, respectively.

Introduction

This chapter summarizes available data on the geometry, structural style, stratigraphic displacement (including both cumulative displacement and individual displacement per faulting event), slip orientation, and chronology of Quaternary faulting events on the Paintbrush Canyon, Bow Ridge, and Stagecoach Road Faults. Because of their close proximity to Yucca Mountain and the proposed repository site for the storage of high-level radioactive wastes (figs. 1, 2), the history and extent of Quaternary surface ruptures along these faults is especially important for estimating paleoearthquake-recurrence intervals and fault-slip rates, as required for seismic-hazard analysis.

Paintbrush Canyon Fault

Paleoseismic investigations were conducted at three sites on the Paintbrush Canyon Fault (fig. 2): (1) at Busted Butte, toward the south end of the fault (Busted Butte walls 1–4); (2) in the central section of the fault (trench MWV-T4); and (3) to the north (trench A1). These exposures, discussed individually below, indicate that multiple Quaternary displacements have occurred on all three sections of the fault.

Busted Butte

The Paintbrush Canyon Fault is well exposed in two 25-m-deep gullies incised into sand ramps that are banked against the west slope of Busted Butte (Whitney and Muhs, 1991). Four of these gully walls (BB-W1 through BB-W4, hereinafter referred to as Busted Butte walls 1 through 4) were cleaned in August 1992 to enhance natural exposures of a succession of buried soils and stonelines displaced by the main fault (figs. 9, 10). Two of these exposures (Busted Butte walls 1, 4) were logged in detail because they contain the most complete stratigraphic record of faulting; the discussion below therefore focuses on the logs and interpretations from these two walls. No fault scarp or other topographic expression of the fault was observed where it crosses broad interfluvial areas between the gullies (fig. 11).

Busted Butte wall 4 contains a west-dipping sequence of 10 unconsolidated lithologic units, including seven buried soils

that represent the most complete stratigraphic succession at the Busted Butte trench site (fig. 9A). Bedrock is exposed locally in the footwall block at the bottom of the gully. The lower part of the sequence consists of thick massive sand layers (units 1–5), which are differentiated primarily on the basis of discontinuous stonelines at lithologic-unit boundaries. These stonelines are associated in places with two weakly developed carbonate soils (S1, S2, fig. 9A). The Bishop ash (760 ka; van den Bogaard and Schirnick, 1995) is preserved near the base of eolian sand-ramp deposits at the south end of Busted Butte, and similar silicic ash is intercalated with sand layers at the base of Busted Butte wall 4 (unit 1, fig. 9A). Thus, the sand ramps in this area chronicle approximately the past 600–700 k.y. of fault-displacement history. Lithologic units in the upper part of the wall (units 6–10, figs. 9, 10) generally are thinner and display greater lateral variations in thickness relative to the lower sand layers. The predominantly sandy deposits in the upper wall also contain coarser gravelly layers that typically mantle the slopes of two distinct buried fault scarps (see below).

Two moderately well developed buried soils (S3, S5, fig. 9) with CaCO₃ stage II–IV morphology (after Birkeland, 1984, and Machette, 1985) and locally abundant rhizoliths are conspicuous features in the upper part of Busted Butte wall 4. Both of these major soils are disrupted by prominent buried fault scarps. Soils continued to development after formation of the scarps, producing zones of silica-carbonate laminae (S3a, S5a) that mantle the scarp slope. At least one thin, poorly developed carbonate soil formed locally on units that bury the fault scarps as well (S4 on unit 7a and S6 on unit 9b, fig. 9B). On other walls, the two conspicuous buried soils are erosionally truncated at or west of the fault beneath weak pavements and thin soils developed on the erosional upper surface of the sand ramps (fig. 10). That type of erosional truncation apparently did not occur on wall 4, possibly in part because there the fault intersected the sand ramp at a site of net deposition downslope from areas of erosional stripping.

The main fault trace is well defined by a 0.2- to 5-m-wide zone of carbonate-coated shears and fractures that commonly increase in complexity upsection (figs. 9, 10). The average orientation and dip of the fault zone in these wall exposures are N. 15° E. and 70° W., respectively. Striations of probable tectonic origin on carbonate-coated shears (N. 11° E., 71° W.) in the sand-ramp fault zone exhibit left-oblique slip with a rake of 73° SW., and slickenlines with left-oblique slip with a rake of 47° were observed in nearby similarly oriented bedrock exposures of the fault (Whitney and Muhs, 1991; Simonds and others, 1995). The slickenside orientation was used to correct for net tectonic displacement because it represents the most direct and unambiguous link to Quaternary fault slip. The hanging-wall block in the upper part of most exposures is deformed by a complex network of minor synthetic and antithetic faults and fractures. Secondary hanging-wall deformation, which approaches 25 m in width in the northernmost exposure (Busted Butte wall 1), includes a small antithetic graben adjacent to the main fault near the top of the wall (fig. 10). On Busted Butte wall 4, two secondary synthetic fault

strands displace sand-ramp units in the footwall block to the east of the main fault trace (fig. 9A).

Structural and stratigraphic relations are summarized below for Busted Butte wall 4 because that exposure provides the most complete record of fault displacements. Successively smaller displacements of younger horizons, fault-generated colluvial wedges, and several buried scarps are interpreted to represent six or seven individual faulting events (table 6) with dip-slip surface displacements per event; factoring in measurement uncertainties, these displacements range from 0 to 246 cm, commonly from 40 to 130 cm (tables 7, 8). All of the six buried soils described above and three additional distinct stonelines are offset along the main fault trace (fig. 9).

The uppermost buried soil (S5, fig. 9) appears to have been displaced by at least two faulting events—most recent event Z and penultimate event Y—that produced colluvial slope deposits 9c and 9b, respectively (fig. 9B; table 8). These units drape downslope across the upper composite fault scarp formed above unit 8e. Event Z deformed and thus postdates a colluvial gravel (unit 9b) with a thin calcic soil (S6) that buried the initial fault scarp and related soil (S5a). The scarp and units associated with event Z were, in turn, buried by several undisturbed gravel or sand deposits that locally are plugged with secondary carbonate (for example, units 9c–9e, fig. 9B). Event Y is interpreted from a set of shears and fractures that displace the scarp and related soil (S5a) but terminate at the base of unit 9b. A possible third faulting event (X) may have produced a small initial paleoscarp (represented by the top of unit 8e) that developed after offsetting of the original buried soil (S5). This paleoscarp was ruptured subsequently by the two later faulting events (Y, Z) to form the composite upper buried scarp. Event X is queried because the composite scarp might have been formed by only events Y and Z. The cumulative vertical displacement of two to three of the latest faulting events affecting the upper buried soil is approximately 1.2 m, as measured by the total offset of unit 7a along all strands of the fault zone below the upper composite scarp (fig. 9B).

The next lower buried soil (S3, fig. 9), developed on unit 6, is displaced by one earlier faulting event (W) that occurred during soil development, causing a dip-slip displacement along the main fault trace of about 1.3 m that is associated with a lower buried fault scarp formed at the top of a colluvial wedge (unit 6e). An additional 25-cm displacement occurred on one of the eastern fault strands as well. The total dip-slip displacement across the main fault strand above and below the lower scarp is 2.2 to 2.5 m, including the cumulative displacement of the three or four faulting events at and above this stratigraphic horizon.

Below the two upper buried soils, two earlier faulting events (T, V) are recorded by carbonate-impregnated colluvial wedges in the midslope to lower slope of the sand ramp (units 4a, 6a, fig. 9A). A third earlier faulting event (U) is indicated in the lower part of the exposure by terminations of fractures beneath a small gravelly channel deposit adjacent to the fault zone (unit 5a, fig. 9A) and by decreasing differential displacements of units 4 and 5.

Minimum estimates of the cumulative dip-slip displacement of the buried stoneline on top of unit 3 (fig. 9B) are estimated to range from 4.3 to 6.7 m (preferred value, 5.1 m); net-slip adjustments increase this range to 4.5–7.0 m (preferred value, 5.3 m). These values were calculated by adding the cumulative offset of the top of unit 4, as measured on the log, to the total displacement from event T that is recorded in a stratigraphically lower colluvial wedge within unit 4 (unit 4a, fig. 9A). This procedure is required because the downthrown equivalent of the unit 3 stoneline is not exposed on the hanging wall. These estimates of the cumulative dip-slip displacement on Busted Butte wall 4 are somewhat larger, but within the same general range, as a dip-slip offset that was measured at the same approximate stratigraphic level on Busted Butte wall 2, where the lowermost soil, which is correlative with the soil horizon on unit 2 exposed on Busted Butte wall 4, is displaced 4 m along the main fault zone (Whitney and Muhs, 1991). This correlation is based on the morphology and relative stratigraphic positions of the soils on the two exposures. The two eastern secondary faults on Busted Butte wall 4 add another 0.9 m of cumulative dip-slip displacement at the stratigraphic levels of units 5 and 6, which, in combination with offsets observed on the main fault strand, yields a minimum estimate of 5.5 to 8.0 m (preferred value, 6.3 m) for the net cumulative displacement on units 1 and 2 at the base of the exposure.

The number and amount of the younger displacements cannot be deciphered clearly on Busted Butte walls 1 through 3 because the stratigraphic record at the fault zone is incomplete, resulting from erosional truncation of soils and units beneath the upper surface of the sand ramps. This problem is especially acute on the footwall block of these exposures. Busted Butte walls 2 and 3 were not logged in detail because of severe erosion of units at upper stratigraphic levels. On the lower part of Busted Butte wall 2, units beneath the lowermost buried soil (S1, fig. 9) are displaced by one or two faulting events (R, S) on a secondary eastern fault strand, although the soil itself is not much offset by that faulting event(s). As noted above, between this exposure and Busted Butte wall 4 the cumulative dip-slip displacement of that soil across the main fault zone is generally consistent. On Busted Butte wall 1, the latest two or three faulting events (X–Z) associated with graben deformation on the main fault zone can be correlated confidently with the faulting chronology of Busted Butte wall 4. Three earlier faulting events (U–W) have been correlated provisionally as well, but those correlations are more difficult because much of the stratigraphic section underlying the graben was stripped from the area now exposed on Busted Butte wall 2, indicating a period of erosion that predates graben formation. Erosion during and after graben development is confined primarily to the footwall block.

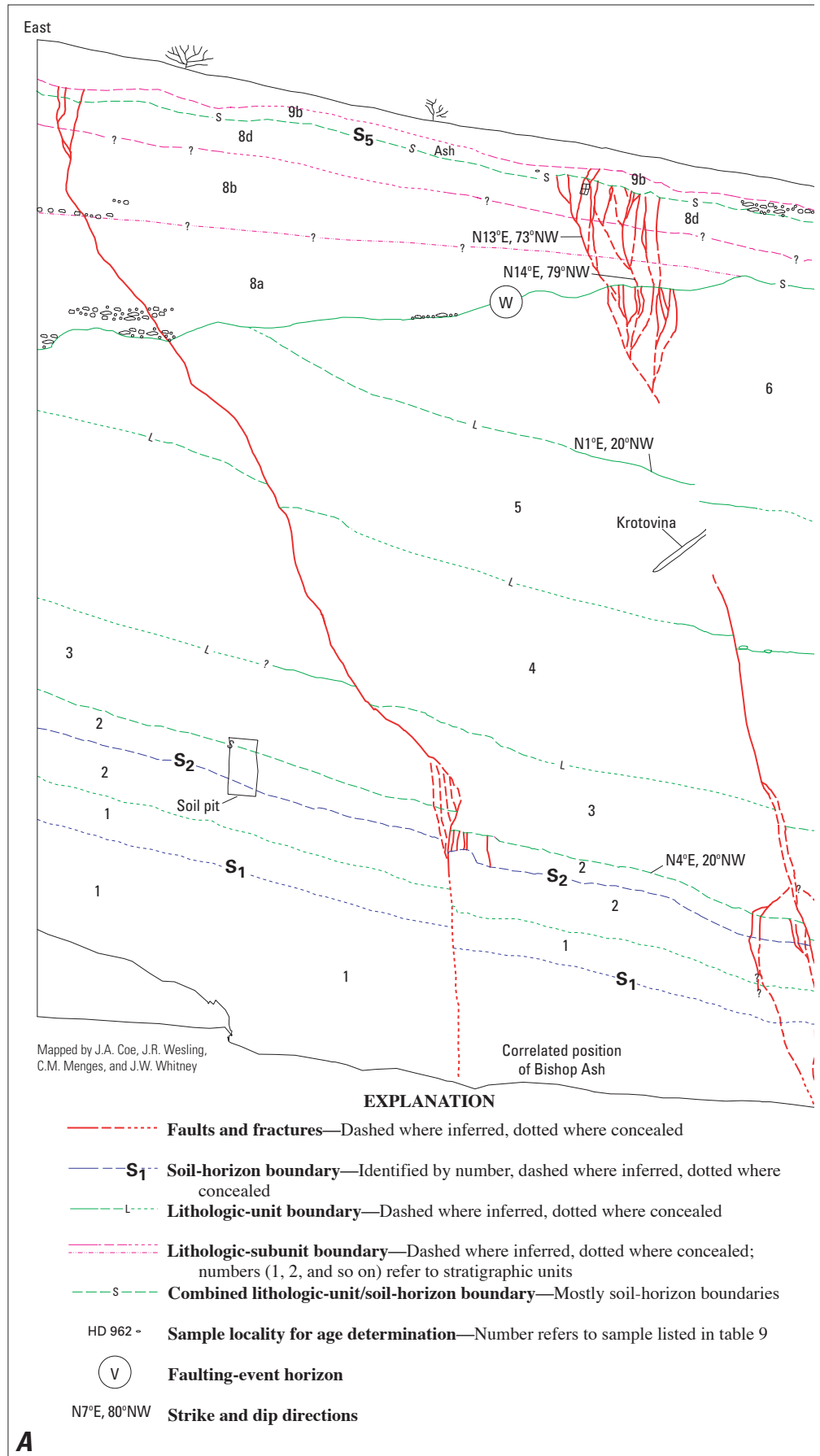
Age constraints on the long paleoseismic record of displacements on the Paintbrush Canyon Fault at the Busted Butte exposures are summarized below.

Earlier events T through V.—A maximum date for events T through V is provided by an approximate maximum age of 650–700 ka for the lowermost buried soil (S1, fig. 9) dis-

placed by these events. This estimate is derived from the stratigraphic position of the soil above the Bishop ash (760 ka; van den Vogaard and Schirnick, 1995) in unit 1 on Busted Butte wall 4 (fig. 9A). A minimum date of approximately 400 ka for this series of faulting events is derived from the estimated age of soil S3 (see below). Individual events in the series cannot be dated because no direct age control exists for units 2 through 6 in the lower and middle sections of the wall that contain events T through V.

Event W.—Event W occurred sometime between the formation of soils S3 and S5 (fig. 9). U-series analyses of pedogenic carbonate laminae collected on Busted Butte wall 4 (sample HD 961, fig. 9A; table 9; Paces and others, 1994) yielded poorly constrained ages of approximately 400 ka for soil unit S3, which predates event W and the formation of the lower buried scarp (unit 6, fig. 9), and of 270 to 300 ka (samples HD 962 and HD 1449, fig. 9A; table 9) for soil unit S5, which is disrupted across the upper fault scarp stratigraphically above this event (top of unit 8, figs. 8, 9).

Possible event X.—The latest two or three faulting events (X?, Y, Z) on the Paintbrush Canyon Fault post-date the formation of soil unit S5 and rhizolith-bearing soils on Busted Butte wall 4 and similar dated soils correlated from Busted Butte wall 1. A suite of rhizoliths in soil S5a that formed along the crest of a scarp on Busted Butte wall 1 yielded U-series ages of about 140 ka (sample HD 955A, fig. 10; table 9), somewhat younger than the cluster of rhizolith ages of 215 to 340 ka from a stratigraphically and lithologically similar unit (8b) in Busted Butte wall 4 (samples HD 962 and HD 1449, fig. 9B; table 9). Thus, the earliest of these faulting events (X?) may have occurred sometime between 300 ka, the approximate age of soil S5 (see above), and before at least the partial development of soil S5a, which has an estimated age of 150 to 300 ka derived from the associated rhizolith ages of units on both Busted Butte walls 1 and 4.



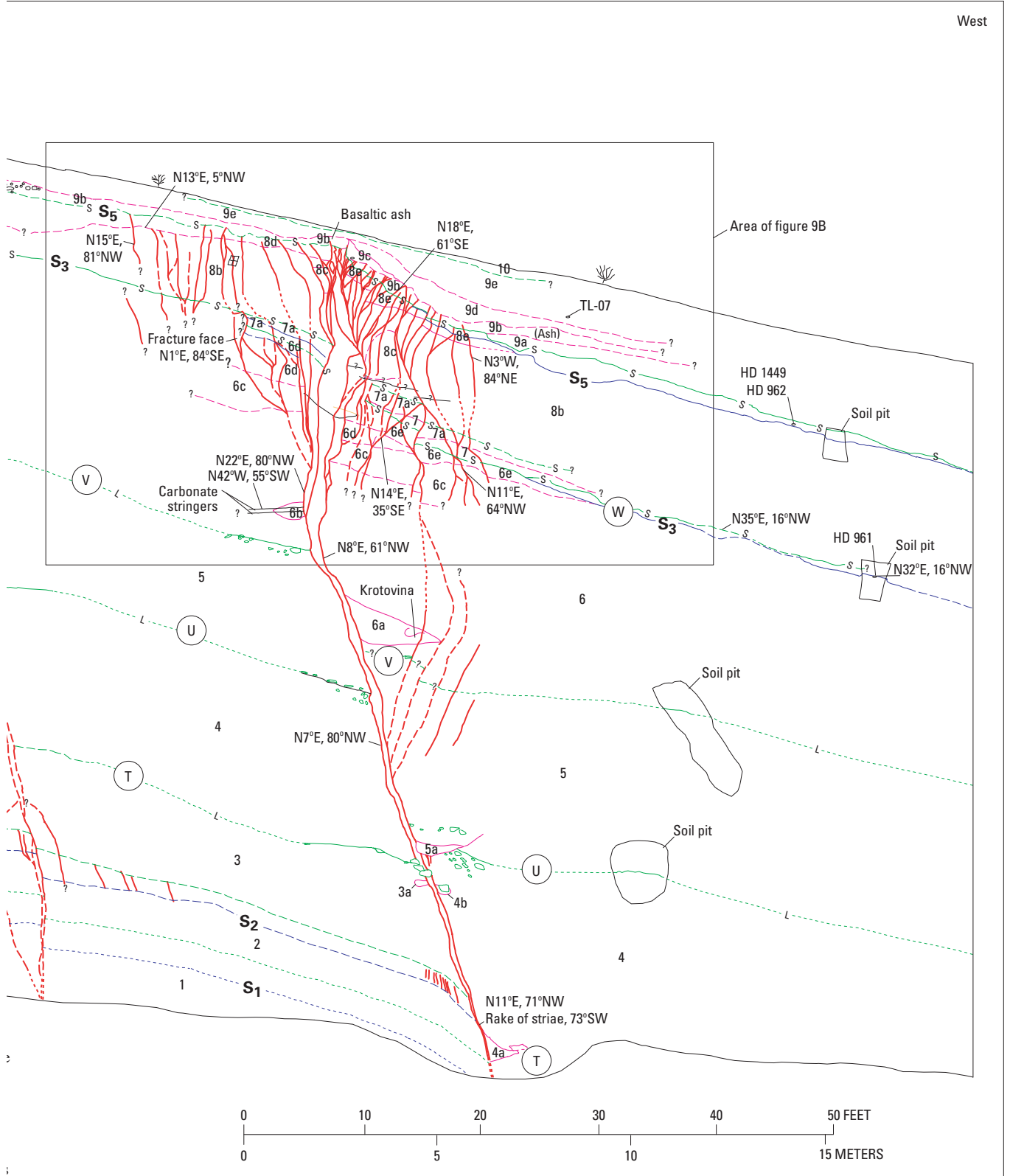
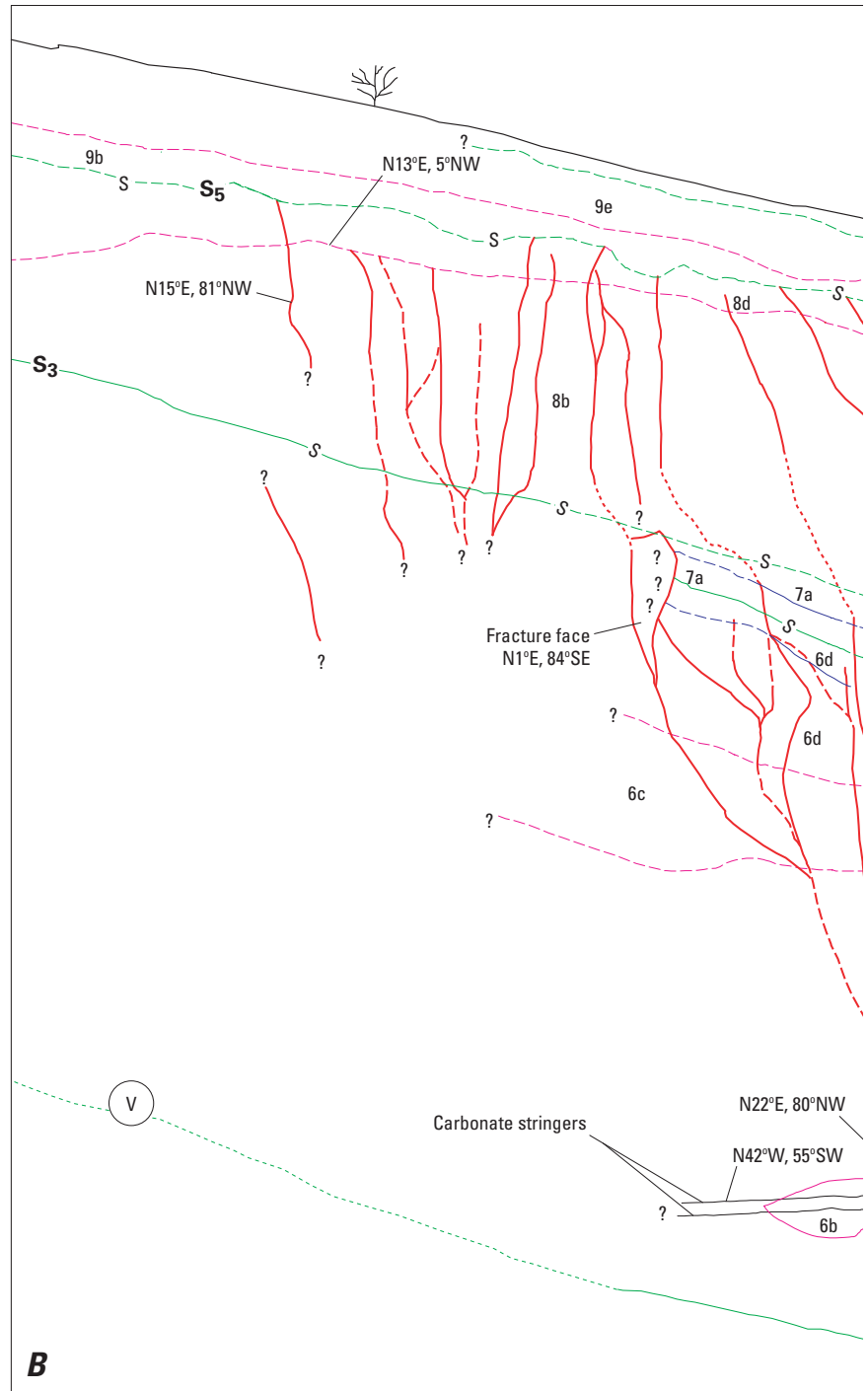


Figure 9. Simplified logs of natural exposures across the Paintbrush Canyon Fault in the Yucca Mountain area, southwestern Nevada (see fig. 1 for locations). A, At Busted Butte wall 4 (BB4, fig. 2). B, In upper part of Busted Butte wall 4.

Penultimate event Y.—The time interval between the development of soils S5a and S6 (fig. 9) brackets the penultimate faulting event (Y). Carbonate laminae with U-series ages of 70 to 80 ka along the fault zone toward the east end of Busted Butte wall 1 (sample HD 954, fig. 10; table 9) are correlated with soil unit S6, which formed on lithologic unit 9b and buried the upper scarp on Busted Butte wall 4 (fig. 9B). These ages, in combination with the broad estimated ages for soil 5a (see above), bracket event Y at approximately 300–80 ka, more likely 150–80 ka (table 10), allowing for uncertainties in the use of minimum ages (of rhizoliths and soils) to constrain event timing.

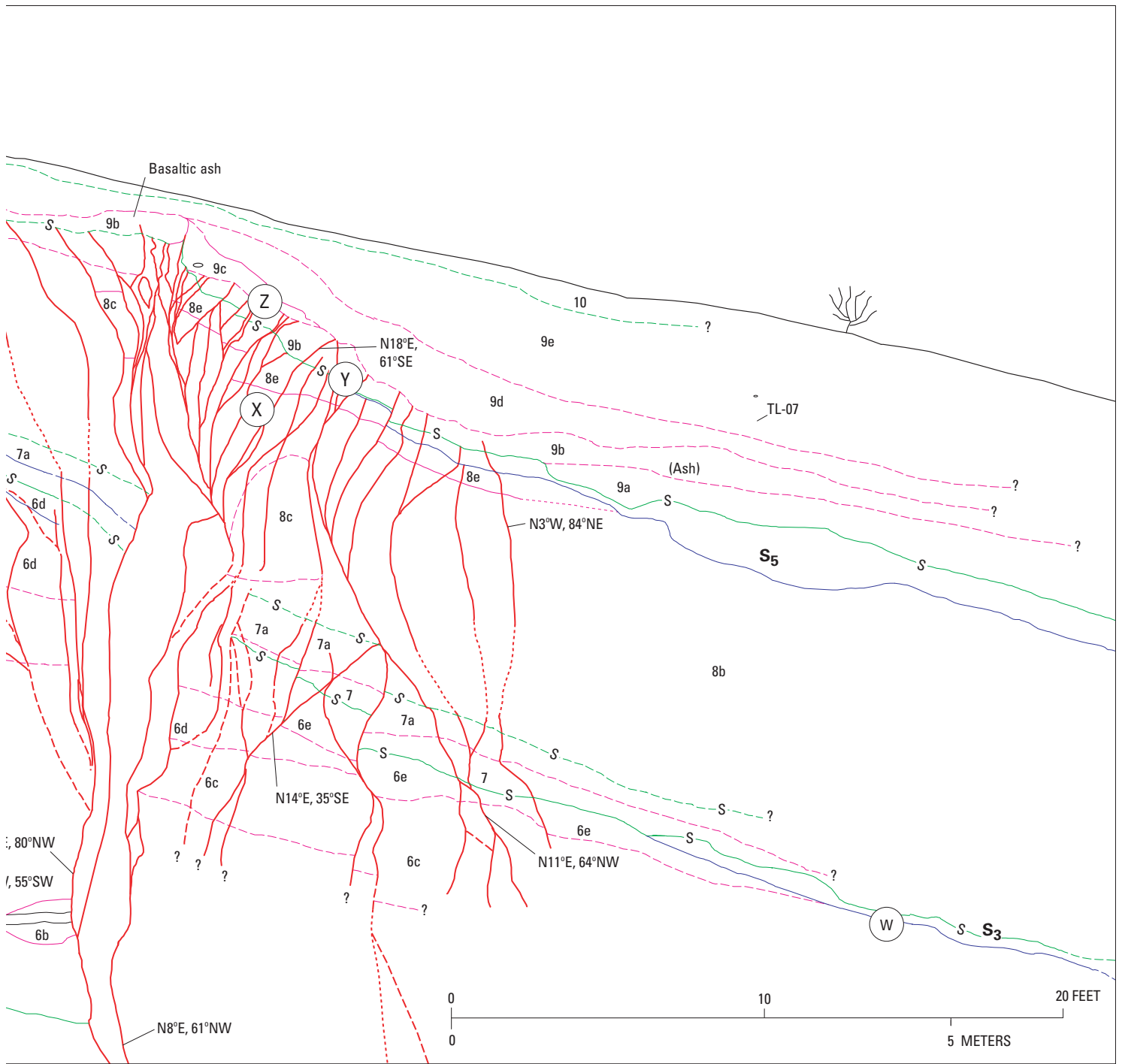
Most recent event Z.—Soil S6 (fig. 9) is displaced only by the most recent faulting event (Z), providing a minimum age constraint for that faulting event. A maximum age constraint is derived from a sand layer (unit 9b, fig. 9B) containing sparse basaltic ash that overlies both the carbonate laminae and upper fault-scarp soil (see events X, Y), and was deposited between events Y and Z. The basaltic ash is correlated provisionally with tephra from the Lathrop Wells basaltic cone south of Yucca Mountain (fig. 1), which is dated by the $^{40}\text{Ar}/^{39}\text{Ar}$ method at about 77 ± 6 ka (Heizler and others, 1999). A minimum age constraint for event Z is provided by unfaulted sand layers, with a thermoluminescence age of 44 ± 13 ka (sample TL-07, fig. 9A; table 9), that bury the fault scarp and postdate all faulting events (fig. 9B). These combined age relations establish a crude age bracket of 80–40 ka for the most recent faulting event (table 10). Fractures related to this event are coated extensively with carbonates, indicating that the most recent surface rupture probably occurred early within this interval (50–40 ka).

The above relations indicate average recurrence intervals ranging from 30 to 270 k.y. (preferred value, 50–120 k.y.) for the complete sequence of recognizable faulting events in the Busted Butte exposures (table 11). Individual recurrence intervals for the three latest faulting events range from 10 to 275 k.y. (preferred value, 65–95 k.y.). Average slip rates of 0.001 to 0.01 mm/yr in mid-Quaternary to late Quaternary time were computed, based on the displacements of three units at different stratigraphic levels (tables 11, 12); the preferred value for the entire sequence is 0.007 mm/yr. Long-term average slip rates computed for the lowermost soil (S1), spanning the entire exposed paleoseismic record, range from 0.008 to 0.01 mm/yr.



Mapped by J.A. Coe, J.R. Wesling, C.M. Menges, and J.W. Whitney.

Figure 9.—Continued



EXPLANATION

- - - **Faults and fractures**—Dashed where inferred, dotted where concealed
- - - **S₃** **Soil-horizon boundary**—Identified by number, dashed where inferred, dotted where concealed
- - - **Lithologic-unit boundary**—Dashed where inferred, dotted where concealed
- - - **Lithologic-subunit boundary**—Dashed where inferred, dotted where concealed; labels (7a, 8c, and so on) refer to numbered subunits

- - - **S** **Combined lithologic-unit/soil-horizon boundary**—Mostly soil-horizon boundaries
- TL-07 **Sample locality for dated material**—Number refers to sample listed in table 9
- (V) **Faulting-event horizon**
- N8°E, 61°NW **Strike and dip directions**

West

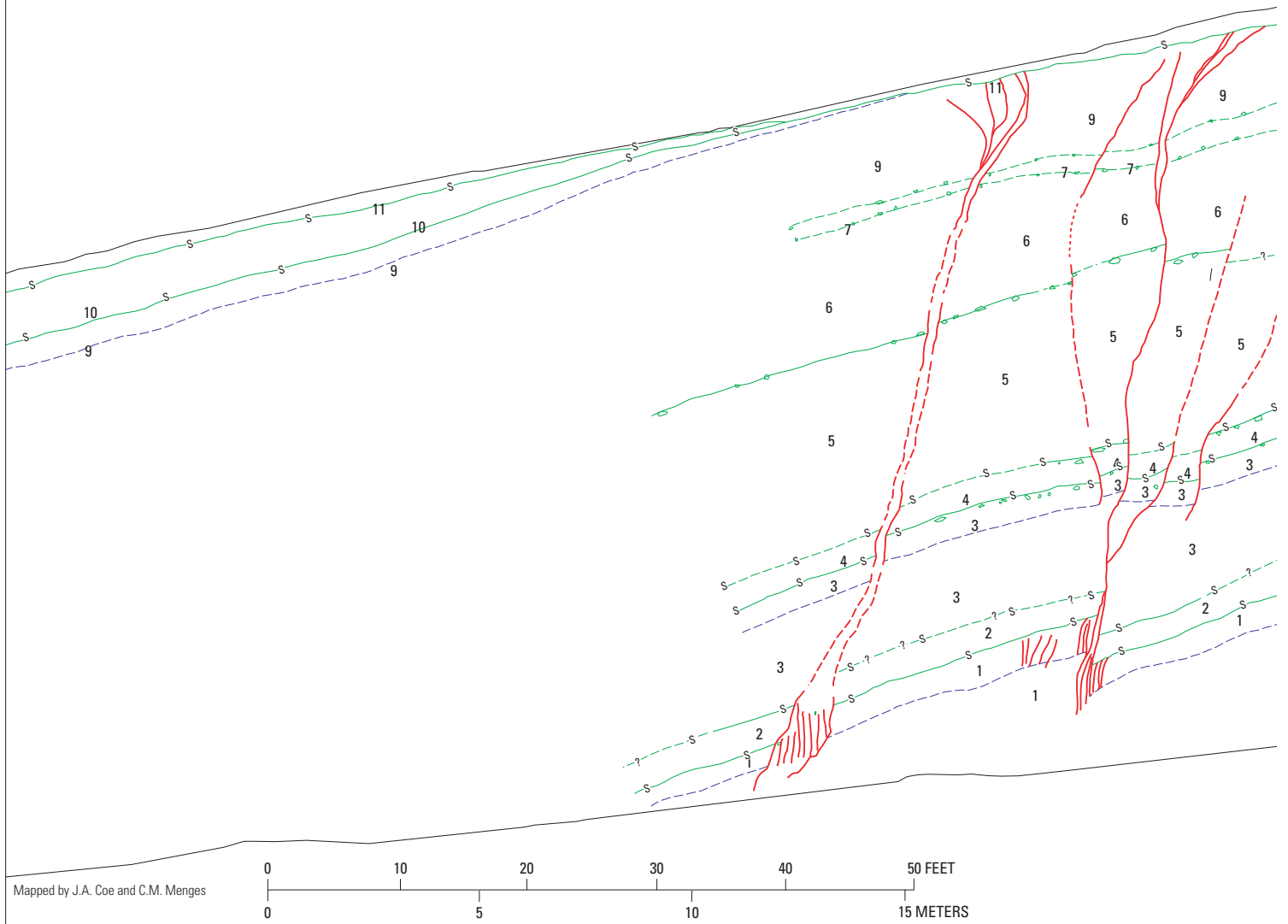
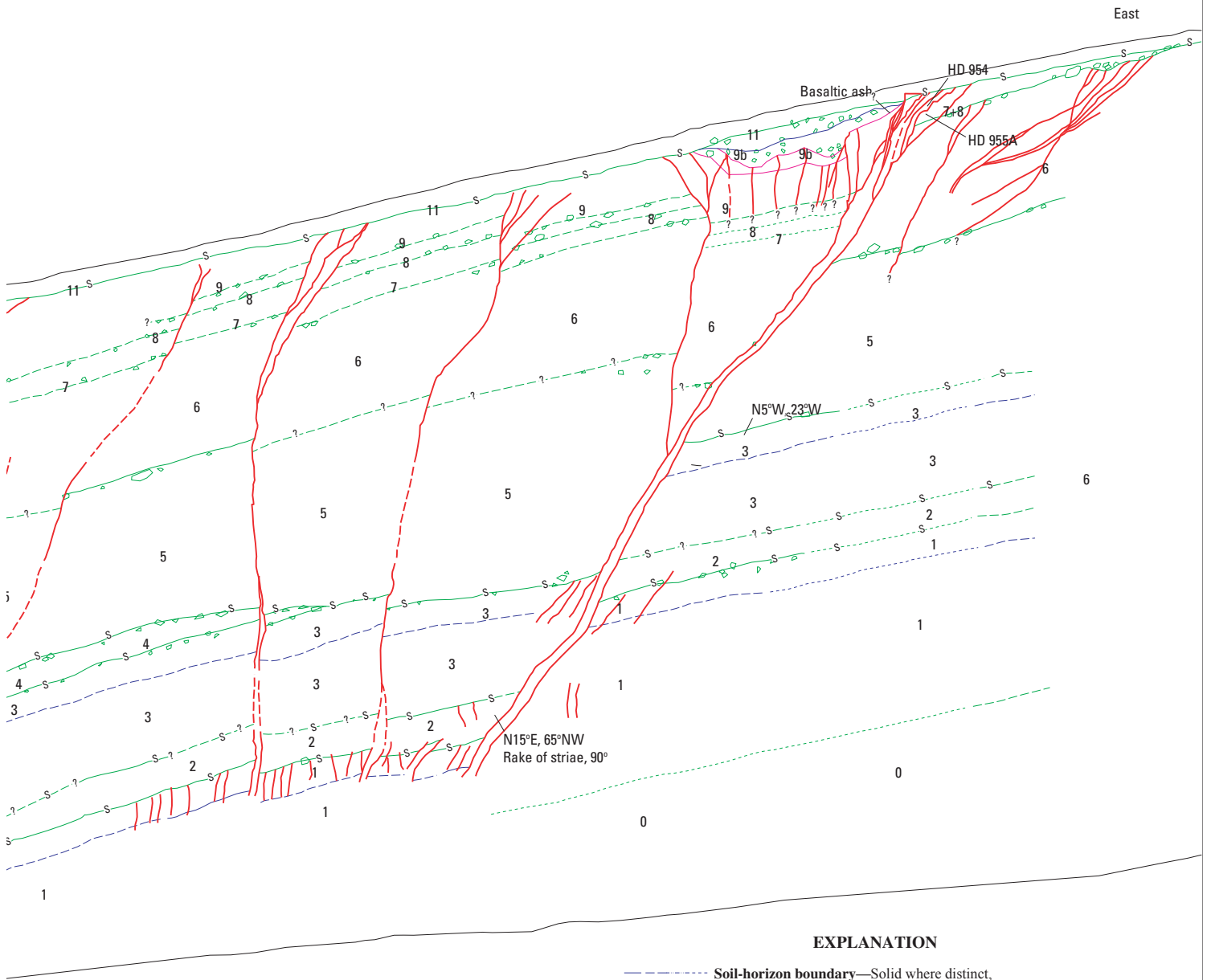


Figure 10. Simplified log of natural exposure across the Paintbrush Canyon Fault at Busted Butte wall 1 (BB1, fig. 2) in the Yucca Mountain area, southwestern Nevada (see fig. 1 for locations).



EXPLANATION

- **Soil-horizon boundary**—Solid where distinct, dashed where inferred, dash-dotted where gradational, dotted where concealed
- **Lithologic-unit boundary**—Solid where distinct, dashed where inferred, dotted where concealed
- **Lithologic-subunit boundary**—Solid line where distinct, dashed where inferred, dash-dotted where gradational, dotted where concealed
- s- **Combined lithologic-unit/soil-horizon boundary**—Mostly soil-horizon boundaries corresponding to lithologic-unit boundaries
- **Faults and fractures**—Dashed where inferred, queried where uncertain
- HD 954 - **Sample locality for dated material**—Number refers to sample listed in table 9
- N35°E, 16°NW **Strike and dip directions**
- 8 **Lithologic unit**

Table 6. Estimated dates and numbers of surface-rupturing paleoearthquakes on the Paintbrush Canyon, Bow Ridge, and Stagecoach Road Faults in the Yucca Mountain area, southwestern Nevada.

[See figure 2 for locations. Date is based on maximum age range of stratigraphic units exposed in hanging wall of trench: eP, early Pleistocene (1,650–775 ka); mP, middle Pleistocene (775–128 ka); lP, late Pleistocene (128–10 ka); H, Holocene (10–0 ka). Age controls: A, basaltic-ash horizon; S, soil stratigraphy; TL, thermoluminescence analysis; U, U-series analysis. Number of events, number of surface-rupturing paleoearthquakes recognized from stratigraphic and structural relations. Criteria for identifying events: D, incremental downsection increase in measurable displacement at event horizon; F, fissure filled with debris at and below event horizon; S, disruption of unit by shearing; T, incremental increase in stratal backtilting; U, upward termination of two or more fractures or shears at event horizon; W, colluvial wedge inferred to be scarp derived]

Trench	Date	Age control	Number of events	Criteria
Paintbrush Canyon Fault				
MWV-T4	H-mP	TL, U, S	3-4	W, S, U
Busted Butte	H-mP	TL, U, S, A	6-7	D, U, S, W
A1	H-m-eP	TL, U, S, A	≥4	D, U, S
Bow Ridge Fault				
T14D	H-mP	TL, U, S	2-3	D, U, S, W, F
Stagecoach Canyon Fault				
SCR-T1	H-lP	TL, U, S, A	2-4	T, U, W
SCR-T3	H-lP	TL, U, S, A	3-5	T, U, W, F

Table 7. Summary of measured displacements on the Paintbrush Canyon, Bow Ridge, and Stagecoach Road Faults in the Yucca Mountain area, southwestern Nevada.

[See figure 2 for locations. All values in centimeters. Individual displacement, dip slip, with most common range in parentheses. Cumulative displacement, dip slip on reference event horizon at base of exposure; direct age control does not exist for all reference units, and so these units do not necessarily correspond to those used for slip-rate calculations in table 12. Net cumulative displacement is adjusted for oblique slip, where possible, and (or) for tectonic rotation or local grabens at fault, where present; absence of reliable oblique-slip indicators in trenches A1 and MWV-T4 adds uncertainty to listed range]

Trench	Individual displacement	Cumulative displacement	Net cumulative displacement
Paintbrush Canyon Fault			
MWV-T4	20-140 (45-65)	170-270	---
Busted Butte wall 4	0-246 (40-130)	≥522-762	≥545-796
A1	0-49	---	>145-170
Bow Ridge Fault			
T14D	¹ 1-46 (12-40)	¹ 30-45, ² 45-70	¹ 33-70, ² 50-122
Stagecoach Road Fault			
SCR-T1	15-105 (40-60)	117-367	99-309
SCR-T3	25-160 (70-105)	153-493	103-299

¹Based on displacement of unit 4 in southern section of trench T14D.

²Based on all measurements of displacements in trench T14D complex, as reported by Menges and others (1997).

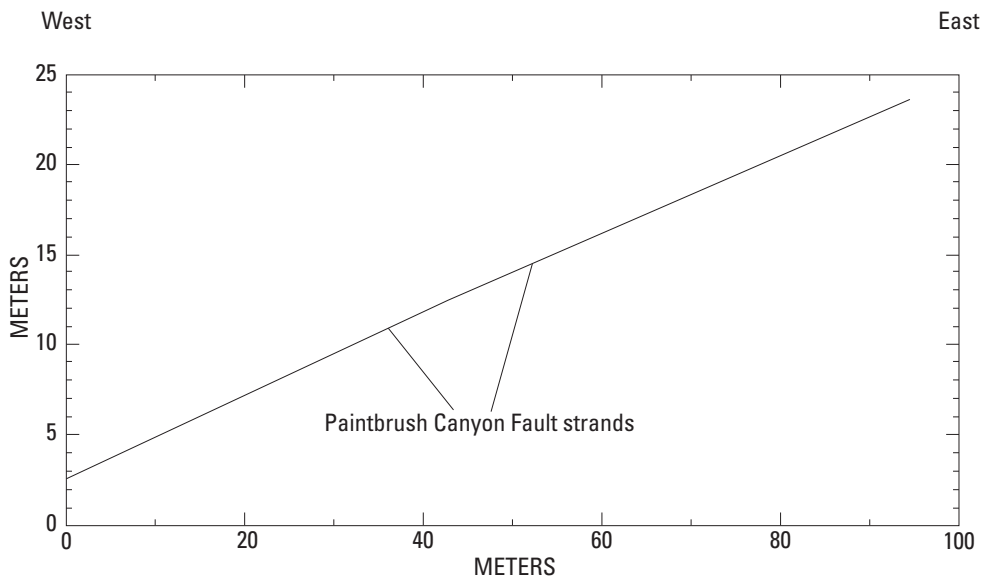


Figure 11. Topographic profile of sand-ramp geomorphic surface on interfluvium across the Paintbrush Canyon Fault above Busted Butte wall 4 on west side of Busted Butte in the Yucca Mountain area, southwestern Nevada (figs. 1, 2).

Table 8. Dip-slip and net displacements for individual faulting events on the Paintbrush Canyon, Bow Ridge, and Stagecoach Road Faults in the Yucca Mountain area, southwestern Nevada.

[See figure 2 for locations. All values in centimeters. Faulting events refer to local chronology at each trench site and do not necessarily imply correlation between sites; faulting events in parentheses are less certain. Dip-slip displacement is measured along fault zone; net displacement is adjusted from dip-slip displacement by including (1) oblique slip, using possible slickenline orientations; and (2) removal of such local deformation effects as backfilling and antithetic graben formation]

Trench	Faulting event	Dip-slip displacement		Net displacement	
		Range	Preferred	Range	Preferred
Paintbrush Canyon Fault					
Busted Butte	Z	0–69	42	0–72	44
	Y	15–54	27	16–56	28
	(X)	33–66	45	35–69	47
	W	84–196	160	88–205	167
	V	0–212	136	0–222	142
	U	12–246	100	12–257	105
	T	72–192	90	75–201	94
MWV–T4	Z	20	20	--	--
	Y	47–77	62	--	--
	X	53–143	98	--	--
	(W)	0–140	40	--	--
A1	Z	--	--	5–10	6
	Y	--	--	29–49	39
	X	--	--	0–14	7
Bow Ridge Fault					
T14D	Z	14–46	40	15–80	44
	Y	4–40	12	4–70	13
	(X)	1–23	13	1–40	14
Stagecoach Canyon Fault					
SCR–T1	Z	40–90	40	40–50	40
	Y	34–84	50	34–70	42
	(X)	15–105	50	28–75	47
	(W)	28–88	60	34–67	51
SCR–T3	Z	60–160	105	41–45	43
	Y	25–100	75	47–79	59
	(X)	30–103	70	49–65	57
	(W)	38–130	100	44–74	67

Table 9. Numerical ages of Quaternary deposits in trenches MWV–T4, A1, T14, and T14D and at Busted Butte in the Yucca Mountain area, southwestern Nevada.

[See figure 2 for locations. Analytical methods used for age determination: Samples: HD (error limits, $\pm 2\sigma$), U-series analyses by J.B. Paces; TL– (error limits, $\pm 2\sigma$), thermoluminescence analyses by S.A. Mahan; YM, U-trend analyses]

Trench or exposure	Sample	Unit and material sampled	Estimated age (ka)
Busted Butte wall 1 (fig. 10)	HD 954	7-8, upper K soil horizon -----	70±28, 77±19, 79±20
	HD 955A	7-8, rhizolith, upper K soil horizon-----	134±23, 137±27, 142±20
Busted Butte wall 4 (fig. 9)	TL–07	9e, sand above upper K soil horizon -----	44±13
	HD 961	8b, lower K soil horizon -----	400+∞/–130, 410+∞/–150
	HD 962	8b, upper K soil horizon -----	300+82/–53, 340+140/–74
	HD 1449	8b, upper K soil horizon -----	272+35/–28
Trench MWV–T4 (fig. 13)	TL–03	VIIe, sand -----	73±9
	TL–04	VIIIb, Bt soil horizon -----	38±6
	TL–05	IX, Av soil horizon -----	6±1
	ND 1368	II, soil carbonate -----	232±15, 344±35
	HD 1370	V?, stringer of opaline silica -----	383±24, 423±44
	HD 1371	VI, rhizolith-----	44±0.5, 55±0.5, 63±1.6
	HD 1372	VI, rhizolith-----	119±2, 131±3
	HD 1372	VI, rhizolith-----	133±5, 140±5
	HD 1589	Ib, opaline silica-----	600+∞/–1±70
Trench A1 (pl. 2)	TL–34	5, Av soil horizon -----	9±1
	TL–35	4c, buried Av soil horizon -----	17±2
	TL–37	2b, sand -----	163±26
	HD 1622	3b, laminar K soil horizon-----	14±2, 16±4
	HD 1623, 1624	2b, rhizolith-----	71±2, 126±7, 195±18, 218±6, 224±21, 266±9
	HD 1625	1b, soil carbonate, opaline silica-----	640+∞/–180, 700+∞/–200, 900+∞/–420
	HD 1627	1b-c, rhizolith -----	403+64/–47, 129±3
	HD 1640	3a, string of opaline silica -----	127±4, 134±5
HD 1641	31-b, rind, stringer of opaline silica -----	85±4, 101±4, 102±4	
Trench 14 (pl. 3)	HD 1A	8S, upper K soil horizon, CaCO ₃ stage IV morphology.	88±5
	YM 14 10–14	8S, laminar carbonate -----	270±90
	YM 14 15–17	7S, sand -----	420±50
	YM 14 18–22	5-6S, basalt gravel in sand-----	488±90
Trench 14D (fig. 16)	TL–06	7a, composite soil sample -----	48±20
	TL–09	4, sand -----	132±23
	HD 968	1, composite soil sample-----	>700
	HD 969	2, composite soil sample-----	340+∞/–120
	HD 970	3b, composite soil sample -----	234+47/–35
	HD 971	5, composite soil sample-----	98±15, 137±32, 139±31, 144±33
Trench SCR–T1 (fig. 19)	TL–02, –26	H1, sand and silt -----	9±1, 12±6
	TL–16	F2b, sand surrounding rhizolith-----	28±4
	TL–25	G2b, sand and silt-----	12±2
	TL–27	D1b, sand and silt-----	49±9
	HD 1067	D1b, rhizolith-----	24±1, 24±2, 25±4, 27±1
	HD 1068	F2b, rhizolith -----	13±6, 17±2, 18±2, 20±2
Trench SCR–T3 (fig. 20)	TL–18	I2-3, sand -----	22±5
	TL–19	G5, sand-----	87±18
	TL–29	G2, sand -----	60±16
	HD 1447	G2, carbonate-cemented sand-----	88±9, 94±35, 104±7, 107±9

Table 10. Estimated dates of selected faulting events on the Paintbrush Canyon, Bow Ridge, and Stagecoach Road Faults in the Yucca Mountain area, southwestern Nevada.

[See figure 2 for locations. Dates: mP, middle Pleistocene (730–128 ka); lP, late Pleistocene (128–10 ka); lsP, latest Pleistocene (40–10 ka); mH, middle Holocene (7–3 ka). MRE, most recent event; PEN, penultimate event. Ash present?, statement whether basaltic ash is present in trench, with stratigraphic position of ash indicated; all ash deposits are provisionally correlated with eruption of the Lathrop Wells volcanic center at 77 ± 6 ka, based on major-ion and trace-element geochemistry, except ash deposit in trench A1, which differs geochemically from ash deposits in other trenches and more closely matches tephra at the Sleeping Buttes volcanic center (B.M. Crowe and F.V. Perry, oral commun., 1996)]

Trench	Date of MRE (ka)	Date of PEN (ka)	Ash present?
Paintbrush Canyon Fault			
MWV–T4	lP (6–40)	lP (70–100)	None recognized.
Busted Butte	lP (40–80)	lP–mP (80–150)	Yes; layer.
A1	lsP (10–20)	mP (130–140)	Yes; fissure, layer (different source?).
Bow Ridge Fault			
T14D	lP (>30–130; ~50)	lP (130–150)	Yes (T14 only); fracture.
Stagecoach Road Fault			
SCR–T1, SCR–T3	mH–lsP (5–15)	lsP (20–30)	Yes; layers.

Trench MWV–T4

Trench MWV–T4 was modified from a preexisting trench excavated across the north end of the western splay of the Paintbrush Canyon Fault that diverges from the main fault strand at the southeast edge of Midway Valley (fig. 2). The trench is located on a short section of the fault associated with low bedrock-controlled scarps (fig. 12). No Quaternary fault activity was reported from studies of the original trench (Swadley and others, 1984); however, the results of more recent reconnaissance work and reviews of existing trenches and geomorphic relations in southern Midway Valley indicated a need to reexamine the fault in that area. Accordingly, the original trench was deepened in June 1992, exposing a distinct fault zone that displaces Quaternary colluvial and eolian deposits (fig. 13).

The main fault trace in trench MWV–T4 (figs. 2, 13) is a 7-m-wide multistrand zone that strikes approximately N. 45°

E. and dips 80° NW. Strands in the western and central parts of the fault zone dip 65°–70° SE. The southeastward dips are considered to be more likely related to local oversteepening of fault strands in the shallow subsurface than to reverse faulting. Secondary fractures and shears are formed in deposits as much as 8 m west of the main fault zone. Faulting in loose friable sand layers (for example, unit VI₁, fig. 13) is expressed as a wide zone of numerous, closely spaced shears and fractures with minimal coatings of silica or carbonate, whereas faulting in moderately to strongly cemented deposits (units II, III, fig. 13) and bedrock is manifested as a narrow zone of discrete silica- and carbonate-plated shears.

The footwall block exposed in the trench contains bedrock (Tiva Canyon Tuff of the Paintbrush Group) thinly mantled with surficial deposits. A well-developed carbonate soil with CaCO₃ stage II–IV morphology is developed on unit II, which overlies bedrock (fig. 13). The hanging-wall block is composed of unconsolidated colluvial and eolian deposits

Table 11. Recurrence intervals and slip rates calculated for the Paintbrush Canyon, Bow Ridge, and Stagecoach Road Faults in the Yucca Mountain area, southwestern Nevada.

[See figure 2 for locations. Average recurrence intervals span two or more faulting events bracketed by age control, with preferred values in parentheses; values for trenches SCR-T1 and SCR-T3 are based on correlation with basaltic ash. Faulting-event chronologies are combined, and so recurrence intervals are identical for trenches SCR-T1 and SCR-T3; average recurrence intervals listed for these two trenches are based on ages determined both by correlation with the Lathrop Wells basaltic ash (A) and by thermoluminescence analysis (TL), with preferred values based solely on ash correlation. Individual recurrence intervals span pairs of successive faulting events with adequate age control; numbers in parentheses, preferred values. Faulting-event pairs used to estimate individual recurrence intervals refer to local chronology at each trench site and do not necessarily imply correlation between sites. Slip rates are calculated from cumulative net slip and age of displaced stratigraphic units, with preferred value in parentheses]

Trench	Recurrence interval (k.y.)			Slip rate (mm/yr)
	Average	Individual		
		Range	Event	
Paintbrush Canyon Fault				
MWV-T4	20–50	40–90 (60)	Z–Y	0.007–0.03 (0.015)
Busted Butte	30–270 (50–120)	25–275 (95) 10–260 (65)	Z–Y Y–X	.001–0.01 (0.007)
A1	50–145 (80–100)	105–130 (115)	Z–Y	.001–0.004 (0.002)
Bow Ridge Fault				
T14D	75–215 (100–140)	40–130 (90) 65–350 (210)	Z–Y Y–X	0.002–0.007 (0.003)
Stagecoach Road Fault				
SCR-T1	A: 18–55 (20–50)	3–78 (10–5) 0–88 (5–50)	Z–Y Y–X	0.02 (0.02)
	TL: 5–50 (10–30)	3–26 (10–2) 0–88 (5–50)	Z–Y Y–X	.02–0.07 (0.05)
SCR-T3	A:18–55 (20–50)	3–78 (10–5) 0–88 (5–50)	Z–Y Y–X	.02–0.03 (0.03)
	TL:5–50 (10–30)	3–26 (10–2) 0–88 (5–50)	Z–Y Y–X	.006–0.04 (0.03)

resembling small sand ramps. The sequence is dominated by poorly bedded to massive sand and silt layers with local gravel accumulations indicative of alluvial channels (for example, units VI, VIIa). Hanging-wall deposits contain several weakly to moderately well developed buried soils characterized by argillic horizons and weak carbonate accumulations with CaCO₃ stage I–II morphology, commonly associated with rhizoliths, that are dispersed in the sandy parent material. The surface soil is thin and weakly developed, with a thin incipient B horizon and carbonate coatings with CaCO₃ stage I–II morphology on gravel clasts.

In the hanging-wall block, the depositional contact between unconsolidated deposits and bedrock (Rainier Mesa Tuff of the Timber Mountain Group) is at a depth of 40 m in a borehole (UE-25p#1) located 40 m north of the trench (Muller and Kibler, 1984). The apparent step in the bedrock-alluvium contact is interpreted to represent the approximate vertical displacement of the top of bedrock across the fault, although some modification of the contact by fluvial erosion cannot be excluded. Structural cross sections indicate that the apparent vertical separation in the Tiva Canyon Tuff across this fault strand is approximately 200 m (Scott and Bonk, 1984).

Table 12. Fault-slip rates calculated for selected dated reference horizons in trenches across the Paintbrush Canyon, Bow Ridge, and Stagecoach Road Faults in the Yucca Mountain area, southwestern Nevada.

[See figure 2 for locations. Number of faulting events is interpreted above reference horizon. Age of reference horizon is determined from geochronologic control. Cumulative net tectonic displacement used to calculate fault-slip rate is derived from measured vertical displacement of reference horizon, adjusted for oblique slip by using slickenlines and (or) local hanging-wall deformation. Values for two trenches (SCR-T1, SCR-T3) across the Stagecoach Road Fault are based on ages determined both by correlation with the Lathrop Wells basaltic ash (A) and by thermoluminescence analysis (TL)]

Trench	Reference horizon	Number of faulting events	Date (ka)	Cumulative net tectonic displacements (cm)		Fault slip rates (mm/yr)	
				Range	Preferred	Range	Preferred
MWV-T4	VIIe	2	73±9	67-97	82	0.007-0.015	0.01
	VII	3-4	<130	170-270	220	.01-0.02	>.015
	VI	3-4	>140	250-350	300	.02-0.03	--
Busted Butte	8a (soil)	2-3	215-350	51-197	119	.001-0.009	.004
	6 (soil)	3-4	270-560	139-402	286	.003-0.015	.007
	3	6-7	600-700	≥525-786	≥608	≥.009-0.01	.009
A1	2b	3	160-275	35-70	45	.001-0.004	.002
T14D (N)	4	2	132±23	30-70	35	.002-0.006	.003
T14D (S)	9	1	109-155	40-80	44	.002-0.007	.003
SCR-T1	A: F2c	2	77±6	138-165	145-155	.04-0.07	.02
	TL: F2b	2	28±4	138-165	145-155	.02	.05
SCR-T3	A: H3c	2	77±6	177-240	205	.02-0.03	.025
	TL: G5a	2-3	87±18	208-255	220-240	.02-0.04	.025

Three or four individual faulting events that postdate unit VI are interpreted from observations in trench MWV-T4 (figs. 2, 13). These faulting events are identified on the basis of colluvial wedges associated with paleoscarps (fig. 13; Swan and others, 1993). The uncertainties primarily arise from the difficulty in accurately identifying this type of wedge in the poorly stratified fine-grained sandy deposits of the hanging-wall block. At least three faulting events are indicated by upward terminations of fractures and shears at three discrete stratigraphic horizons as well. One or two faulting events (W, X) occurred in the central part of the

shear zone, on the basis of the presence of several colluvial wedges (units VIIb, VIIc, fig. 13). Ambiguity results from uncertainty over whether the two wedges represent individual faulting events (the preferred interpretation) or are simply parts of a single composite wedge. The two most recent surface ruptures are on the easternmost main fault shear. Unit VIIe is considered a scarp-derived colluvial wedge from the penultimate faulting event (Y), and unit IX thickened across the fault after the most recent surface rupture of unit VIIIb in event Z. Another faulting event could be interpreted on the westernmost fault strand, on the basis of the presence of a colluvial wedge (unit VIIa, fig. 13); however, the deposition of this unit is considered to be more likely in response to a faulting event on the central fault strand (event W or X), rather than related to a separate, discrete surface rupture on the western fault strand.

Minimum individual dip-slip displacements, which were estimated from the differential cumulative displacements of successive units and thickness of colluvial wedges, range from 20 to 140 cm, typically from 45 to 65 cm (table 7). The largest displacement is interpreted from the two overlying colluvial wedges (units VIIb, VIIc, fig. 13) to be associated with a single surface rupture. The most recent surface rupturing event has the smallest displacement, approximately 20 cm (tables 7, 8). Estimated cumulative dip-slip displacement of the oldest surficial deposit in the trench ranges from 170 to 270 cm (table 7); these values could not be adjusted for net slip because no slip indicators were observed in the trench.

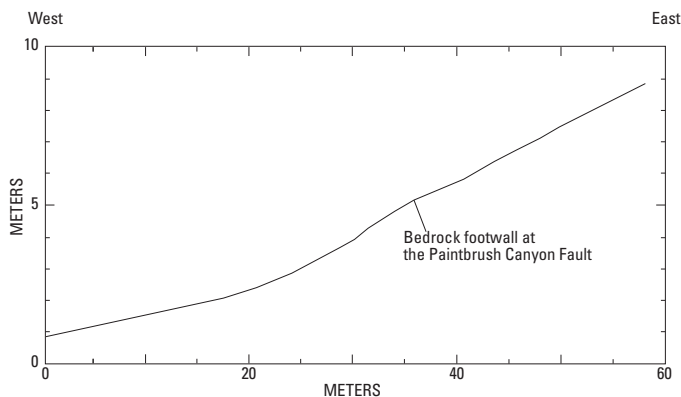


Figure 12. Topographic profile of colluvial footslope south of trench MWV-T4 in the Yucca Mountain area, southwestern Nevada (figs. 1, 2).

Displaced surficial deposits are correlated with the middle to upper Pleistocene alluvial deposits mapped in Midway Valley and vicinity (Swan and others, 1993; Wesling and others, 1992; S.C. Lundstrom, written commun., 1993). The available geochronologic data for dating faulting events on the Paintbrush Canyon Fault in trench MVW-T4 (figs. 2, 13) are as follows:

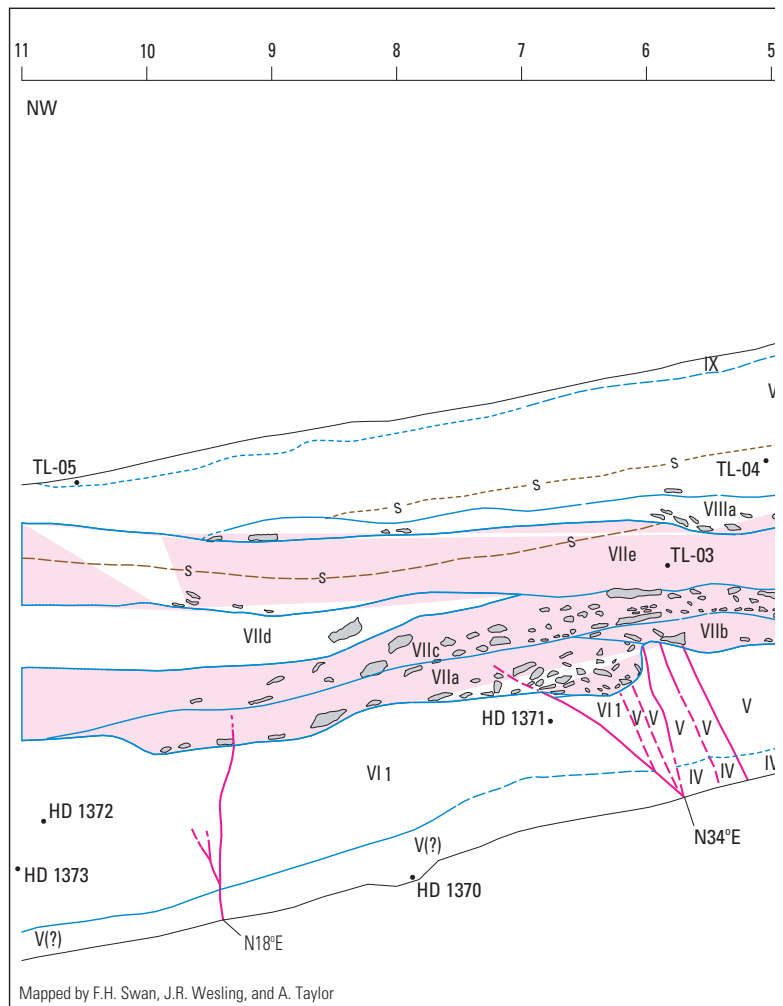
1. The oldest unit is a series of highly cemented and deformed deposits in the fault zone with a U-series age of approximately 600 ka (unit I; sample HD 1589, fig. 13; table 9). The carbonate soil on unit II, which overlies bedrock on the footwall block, yielded U-series ages of 232 ± 15 and 344 ± 35 ka (sample HD 1368). Opaline stringers in unit V, a cemented sandy layer at the base of the trench on the hanging-wall block, yielded U-series ages of 383 ± 24 and 423 ± 44 ka (sample HD 1370).
2. The overlying unit (VI₁), contains numerous rhizoliths with U-series ages ranging from 44 ± 0.5 to 140 ± 5 ka (samples HD 1371, HD 1372, HD 1373, fig. 13; table 9). The oldest of these ages is considered an approximate minimum age for the unit, although the deposit itself could be older than any of the rhizoliths. The minimum rhizolith ages from this unit provide a lower age constraint on the main sequence of late Quaternary faulting events (W-Z) recognized on the hanging-wall block.
3. Two thermoluminescence analyses provide additional age controls for the youngest two identified surface ruptures. A colluvial wedge associated with penultimate event Y (unit VIIe, fig. 13) yielded a thermoluminescence age of 73 ± 9 ka (sample TL-03, table 9), which represents a close minimum for the faulting event itself.
4. The most recent surface rupture (event Z) cuts a mixed eolian-colluvial unit (VIIIb, fig. 13) that yielded a thermoluminescence age of 38 ± 6 ka (sample TL-04). A thermoluminescence age of 6 ± 1 ka (sample TL-05) was obtained on a young surface Av soil horizon that formed on top of unit VIIIb, as well as on unit IX. Neither the soil nor unit IX is cut by event Z, which brackets the most recent faulting event at this site between approximately 40 and 6 ka.

These ages collectively indicate average recurrence intervals ranging from 20 to 50 k.y. (table 12), with individual recurrence intervals ranging from 10 to 75 k.y. The long interval is associated with events Z and Y, whereas the short intervals are estimated for events Y, X, and, possibly, W, which are separated by colluvial wedges with little or no soil development (Swan and others, 1993). The observed net displacement of 67 to 97 cm on unit VIIe with the older thermoluminescence age of 73 ± 9 ka indicates a poorly constrained preferred slip rate of about 0.01 mm/yr (table 12). Slip rates calculated for units VII and VI, using the oldest minimum rhizolith ages, range from 0.01 to 0.03 mm/yr (preferred value, 0.015–0.025 mm/yr).

Figure 13. Simplified log of section of north wall of trench MVW-T4, which exposes western splay of the Paintbrush Canyon Fault in the Yucca Mountain area, southwestern Nevada (figs. 1, 2).

Trench A1

The Paintbrush Canyon Fault is exposed in colluvium in trench A1, which is located on the north end of Alice Ridge at the northeastern margin of Midway Valley (fig. 2). No fault scarps or other direct surface expressions of the fault were observed in that area (fig. 14). Both this trench and an adjacent trench (trench A2, fig. 2) were originally excavated in 1979. Mapping of the north wall of trench A1 at that time revealed carbonate-filled fractures, but no faults or discrete displacements were described (Swadley and others, 1984). No deformation was observed in the terrace gravels exposed in trench A2. In December 1993, new excavations were initiated to provide evidence for the northward extent of surface rupture on the Paintbrush Canyon Fault zone in the northern Midway Valley-Yucca Wash area. Trench A1 was deepened and extended to its present length of 110 m, thereby clearly exposing a complex fault zone in mid-Quaternary to upper Quaternary deposits. An additional 1.5-m-deep backhoe trench, or slot, also was cut into the floor of the main trench across the main fault trace (pl. 2). Another trench (MWV-T3, not shown in fig. 2) that was excavated at that time across a vegetation lineament to the west of trench A1 exhibited no fracturing or



fault deformation and was not logged. The absence of deformation in that trench indicates that Quaternary surface rupture on the Paintbrush Canyon Fault is constrained to the relatively narrow fault zone visible in trench A1.

Trench A1 (fig. 2) exposes a nearly 5-m-thick section of alluvial, colluvial, and eolian deposits; 15 individual depositional layers were recognized and grouped into five soil-stratigraphic units (pl. 2). Most of units 2 through 5 in the upper and middle parts of the trench consist of sand and silt, with a varying, somewhat localized component of pebble-cobble gravel. Coarser grained pebble-boulder gravel predominates in unit 1 in the bottom of the trench. Basaltic ash is dispersed in a silt pod and a fissure fill in the fault zone within the inner slot of the trench. Ash within the fissure fill is restricted to a zone adjacent to the ash-bearing pod. This pod, which appears to be stratabound at the base of unit 2, is buried beneath more than 3 m of sediment.

Each of the principal soil-stratigraphic units contains a distinctive soil presumed to have formed during a period of surface stability. The degree of soil development ranges from weak Bw cambic soils near the surface to Btk horizons containing carbonate accumulations with CaCO₃ stage II–III morphology that locally reach K-horizon cementation in unit 1

(fig. 9). Throughout the entire length of the trench, individual depositional layers pinch out and change in characteristics laterally, reaching maximum thicknesses within the fault zone at the footslope position of the hillslope. Soil horizons likewise vary laterally and merge upslope and downslope from an area of maximum differentiation near the fault zone.

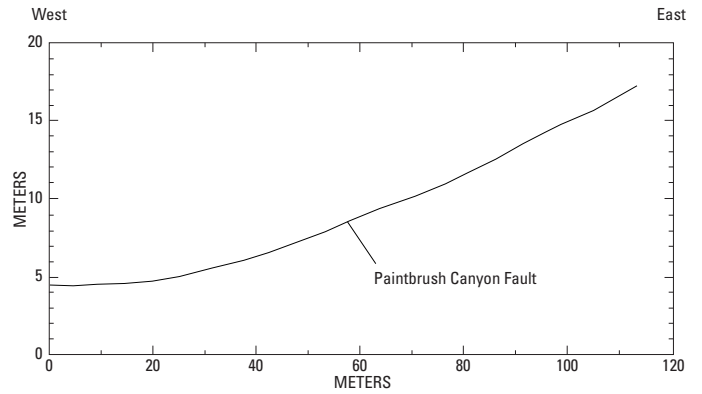
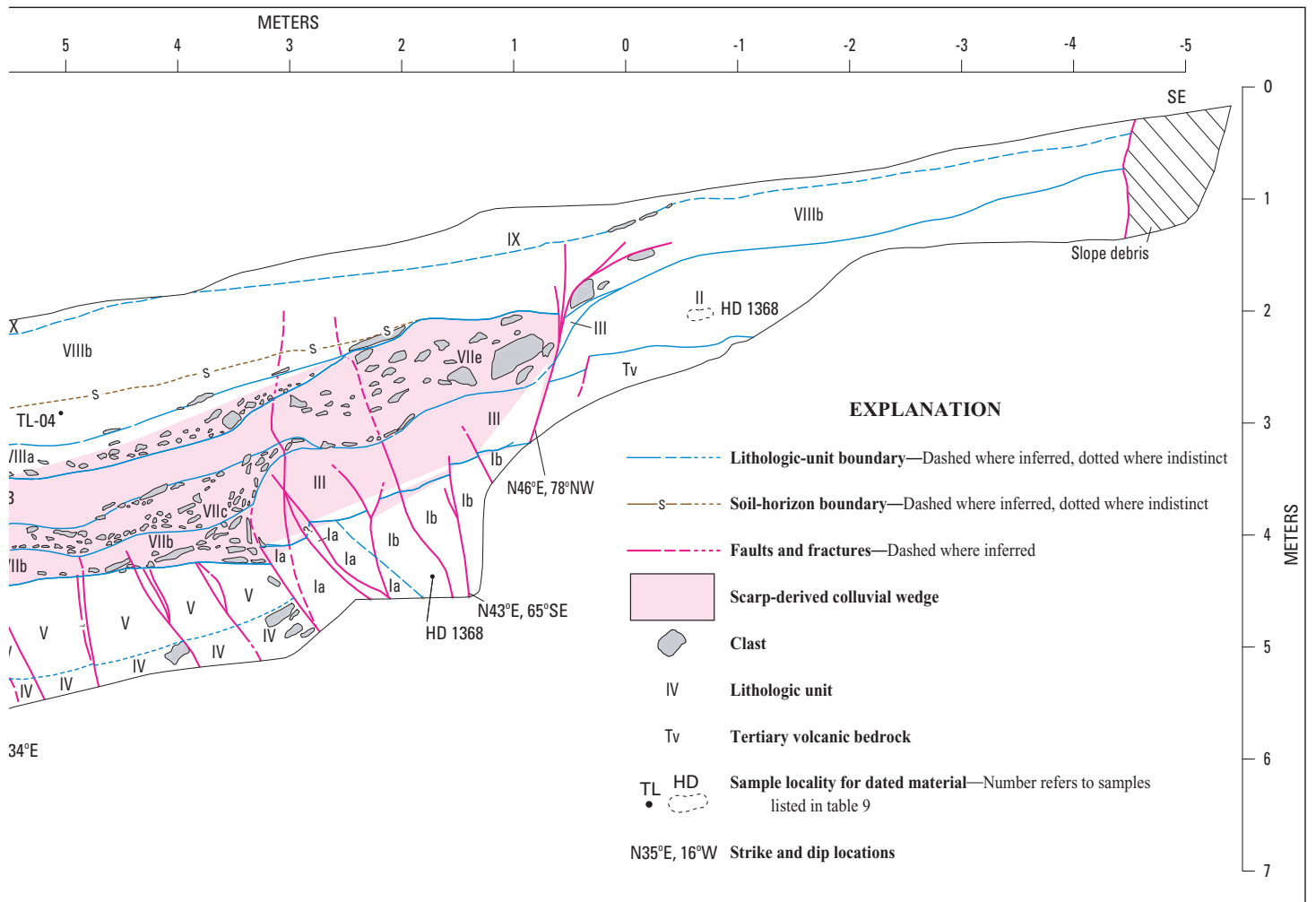


Figure 14. Topographic profile of colluvial footslope at north edge of trench A1 in the Yucca Mountain area, southwestern Nevada (figs. 1, 2).



Trench A1 (fig. 2) exposes a 15-m-wide multiple-strand fault zone that records at least four Quaternary faulting events (see pl. 2). The zone contains a complex array of synthetic and antithetic high-angle normal faults, fractures showing no apparent displacement, and low-angle thrust faults; however, most of the displacement is concentrated on two fault strands (B, C/D, pl. 2), approximately 2 m apart, that compose the main fault zone. These fault strands strike N. 17°–23° E., with predominantly subvertical dips (85° E.–85° W.), although both strands develop upsection into principally east dipping low-angle splays. The lowermost exposed 3 m of the fault zone is characterized by carbonate-engulfed fractures and shears and zones of loose breccia, as much as 50 cm wide, that may represent either broad shear zones or a series of fissure fills, or both. Subsidiary fault strands and fractures that are both east and west of the main fault zone are characterized by carbonate-filled fractures and shears. Many of the fractures show no apparent displacements. Small antithetic east-side-down displacements are present on two fault strands (A, F, pl. 2). Strand C/D has several low-angle east-dipping thrust-fault splays that sole into the main fault zone near the bottom of the trench. Such geometry probably is related to accommodation of local stresses caused by shallowing of the dip on the main fault zone at depth, and (or) a component of strike-slip displacement. No striations or slickensides were observed that could establish the presence or amount of lateral slip, although changes in thickness of some units on opposite sides of the fault zone probably indicate a component of lateral slip.

At least four faulting events are interpreted on the Paintbrush Canyon Fault at trench A1 (fig. 2; table 6). The main criteria used to define these events are (1) progressively smaller vertical displacements of successively younger stratigraphic units and (2) upward terminations of fractures and fissure fills at a given stratigraphic horizon. Small scarp-derived colluvial wedges that are associated with the penultimate faulting event (Y, table 8) are interpreted from unit 1, although wedge features are difficult to recognize because of small displacements and the massive fine-grained texture of many deposits. Evidence for the earliest faulting event (W) is interpreted from unit 1 on the basis of incremental increases in the offset of the unit and possible fault-scarp colluvium. Event W probably includes multiple surface ruptures that cannot be differentiated individually, owing to poor stratigraphic control in the trench. Evidence for event X is the most equivocal, consisting mainly of a few fracture terminations at the interpreted event horizon (top of unit 2c, fig. 9), a slight increase in displacement at the horizon, and a possible fissure-fill unit. In contrast, penultimate event (Y) is well defined by widespread fracture and shear terminations at the top of unit 3c, by differential displacement that on many strands ends at the event horizon, and by a possible small colluvial wedge within unit 3c. The most recent event (Z) is less conspicuous but is clearly indicated by a small displacement of units 4a through 4c (fig. 9) and by fracture terminations.

All of the vertical displacements are small, ranging from 0 to 49 cm for the three recognizable individual faulting events

(tables 7, 8). The smallest net displacements are associated with events X and Z (preferred displacements, 7 and 6 cm, respectively), whereas net displacements resulting from penultimate event (Y), which are distributed among all of the fault strands with observed offsets, are estimated to range from 29 to 49 cm (preferred value, 39 cm; table 8). The minimum net cumulative vertical separation measured at the lowest event horizon (W) in the trench is 145 to 170 cm on the two walls. Displacements per event are generally higher on the north wall and considered more representative than those on the south wall.

The deposits exposed in trench A1 range in age from early(?) through middle Pleistocene to Holocene, on the basis of a series of U-series and thermoluminescence ages (table 9) in combination with general soil-stratigraphic relations (pl. 2). Carbonate from petrocalcic soil in the stratigraphically lowest alluvial deposits (unit 1c, pl. 2) at the base of the slot trench yields poorly constrained U-series ages ranging from 640 to 900 ka (sample HD 1625, table 9); these deposits are overlain by carbonate-cemented gravel layers with silica rinds on clasts that contain excess Th and are depleted in ^{234}U . Rhizoliths from the same general interval in unit 1b in the slot trench yield minimum U-series ages of 129 ± 3 and $403+64/-47$ ka (sample HD 1627). Unit 1, which predates all of the interpreted events in the trench, has an age of at least 750 ka, based on slip-rate constraints (see below). Unit 2b (pl. 2) contains a series of rhizoliths with U-series ages ranging from 71 ± 2 to 266 ± 9 ka (samples HD 1623, HD 1624, pl. 2; table 9), mostly from 220 to 230 ka. One sample (TL-37) with a thermoluminescence age of 163 ± 16 ka that was also collected from this unit is considered to represent a minimum age that is related to postdepositional translocation of silt during soil formation. The probable age of unit 2b is 220–275 ka. Event X, which is above unit 2b within the same soil-stratigraphic unit, probably does not significantly postdate the minimum estimated age for unit 2b. A minimum date for penultimate event (Y) is based on U-series ages of 127 ± 4 to 134 ± 5 ka (sample HD 1640) from a carbonate stringer precipitated along a fracture created by the event. Assuming that carbonate accumulates rapidly within an open fracture, these ages provide a close minimum date and, within analytical error, likely approximate the date of event Y. Laminae and clast rinds from the overlying upper calcic horizon in unit 3b yielded U-series ages ranging from 14 ± 2 to 102 ± 4 ka (samples HD 1622 and HD 1641, respectively, pl. 2; table 9), illustrating that calcic soils commonly provide only crude minimum age constraints. The most recent event (Z) is closely bracketed between unfaulted unit 5, with a thermoluminescence age of 9 ± 1 ka (sample TL-34), and the underlying displaced unit 4c, with a thermoluminescence age of 17 ± 1 ka (sample TL-35).

The age and source of the basaltic ash in the slot trench are potentially problematic. The ash-bearing units, including the fissure fill, appear to be stratabound beneath unit 2b (with a minimum age of 220–275 ka); however, the ash might extend higher upsection in a fissure outside the plane of the trench walls. Given these relations, the eruption of the nearby Lathrop Wells volcanic center at 77 ± 6 ka (Heizler and others, 1999) does not appear to be a likely source for the ash. A pos-

sible alternative source vent consistent with the age constraints in trench A1 is the Sleeping Buttes volcanic center, approximately 40 km to the northwest, which has yielded K-Ar ages of 350 ka (Crowe and others, 1995). Preliminary geochemical analyses of the ash in trench A1 support this correlation with the Sleeping Butte tephra and are not consistent with a source from the Lathrop Wells volcanic center.

Recurrence intervals calculated from these age data range from 50 to 145 k.y. (preferred value, 80–100 k.y.; table 11). The individual recurrence interval between events Y and Z is relatively long, about 105–130 k.y. Fault-slip rates computed from 35 and 70 cm of cumulative dip-slip displacement of unit 2b, with an age of 160–275 ka, range from 0.001 to 0.004 mm/yr (preferred value, 0.002 mm/yr; tables 10, 11). These low rates primarily reflect the small displacements observed at the trench site.

Bow Ridge Fault

The two trenches (T14, T14D, figs. 2, 8) discussed in this chapter are part of a series of five trenches excavated across the surface trace of the Bow Ridge Fault at the west base of Exile Hill, about midway along the mapped north-south length of the fault (see Day and others, 1998a). Trench T14 was excavated in 1982, and preliminary mapping was completed by Swadley and others (1984). Though exposing a well-defined fault zone, the trench provided sparse and poorly resolved data on the amount and timing of late Quaternary fault movements. The excavation, however, yielded valuable information on the composition and origin of the secondary carbonate and silica veins in the fault zone, as described below.

Trench T14 was deepened, and four new trenches (T14A–T14D, fig. 2) were excavated, in 1985 to better define the Quaternary displacement history of the Bow Ridge Fault. The fault zone exposed in trenches T14A and T14B is entirely within bedrock (Tiva Canyon Tuff), and so neither trench was logged. Trench T14C was logged, but paleoseismic relations are obscure because of poorly defined Quaternary stratigraphy, overprinting by pedogenic carbonate, and the absence of discrete vertical displacements on the fault that can be tied to specific marker horizons (Menges and others, 1997).

In 1992, trench T14D was extended 40 m eastward, for a total length of 50 m, to investigate whether another Quaternary strand of the Bow Ridge Fault exists in bedrock at the west base of Exile Hill. A box network of auxiliary trenches, 7 m on a side, also was excavated around the main fault zone north of the west end of trench T14D in an attempt to gain three-dimensional exposures of displaced Quaternary deposits. Results of the mapping of this complex of trenches are summarized below.

Trench T14D

Trench T14D (fig. 2) contains a vertical succession of lower Pleistocene to Holocene deposits along the western margin of Exile Hill; no fault scarp or other topographic expres-

sion was observed along this part of the Bow Ridge Fault (fig. 15). Bedrock of the Miocene Tiva Canyon Tuff is exposed only in the eastern section of the trench, 15 m east of the main fault zone. The tuff is overlain by carbonate-engulfed colluvial fragments that are buried, in turn, by 1.5 to 2 m of surficial deposits representing a westward-thickening sequence of mixed alluvial, colluvial, and eolian origin that has been subdivided into 8 to 16 lithologic units (figs. 16, 17). Most of the units consist of fine- to medium-grained silty sand to sandy silt, with varying proportions of pebble-cobble gravel and local gravelly debris-flow and alluvial-channel deposits. These deposits generally are unconsolidated to moderately cemented, very poorly sorted, and poorly bedded to massive.

Deposits in the west end of trench T14D contain a complex sequence of weakly to moderately well developed soils, including a vertically stacked to partly overlapping series of two to five buried paleosols below a thin surface soil. The buried soils are moderately well to well developed and consist of carbonate and silica accumulations (Bkq to Kq horizons containing carbonate with CaCO_3 stage II–IV morphology) or argillic (Bt or Btk) horizons. The surface soil is relatively thin and weakly developed, consisting mostly of a Bw or weak Bt horizon above a Bk horizon containing carbonate coatings with CaCO_3 stage I morphology on clasts.

The main Bow Ridge Fault trace in trench T14D is characterized on the lower part of the trench walls by a distinct, but irregular, 20- to 40-cm-wide shear zone (figs. 16, 17) that strikes N. 5°–15° E. and dips 80°–85° SE., indicative of slight oversteepening of the fault in the direction of the downdropped block. This oversteepening is probably a near-surface phenomenon, inasmuch as subsurface data indicate steep northwestward dips at depth, as noted above. Multiple veins and laminae of secondary carbonate and silica coat the walls of the shear zone. Several sets of striations on carbonate laminae in the main fault zone, if tectonic in origin, indicate left-oblique slip plunging 35°–65° SE. Three sets of fissures have formed along the main fault trace in the northern section of trench T14D (for example, units F1–F3, fig. 16). The fissures are filled with sand, silt, and

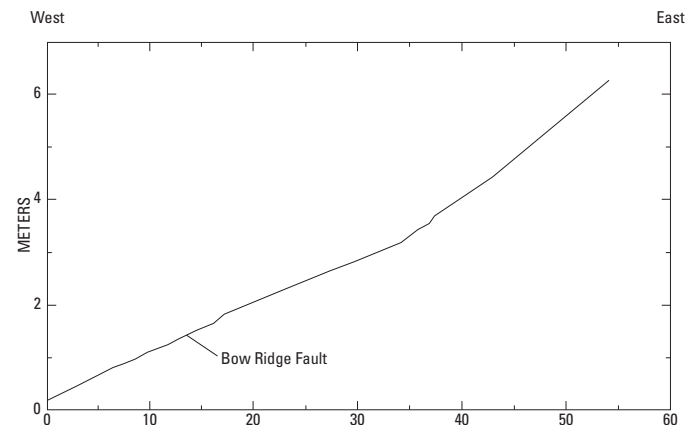


Figure 15. Topographic profile of colluvial footslope across the Bow Ridge Fault south of trench T14D in the Yucca Mountain area, southwestern Nevada (figs. 1, 2).

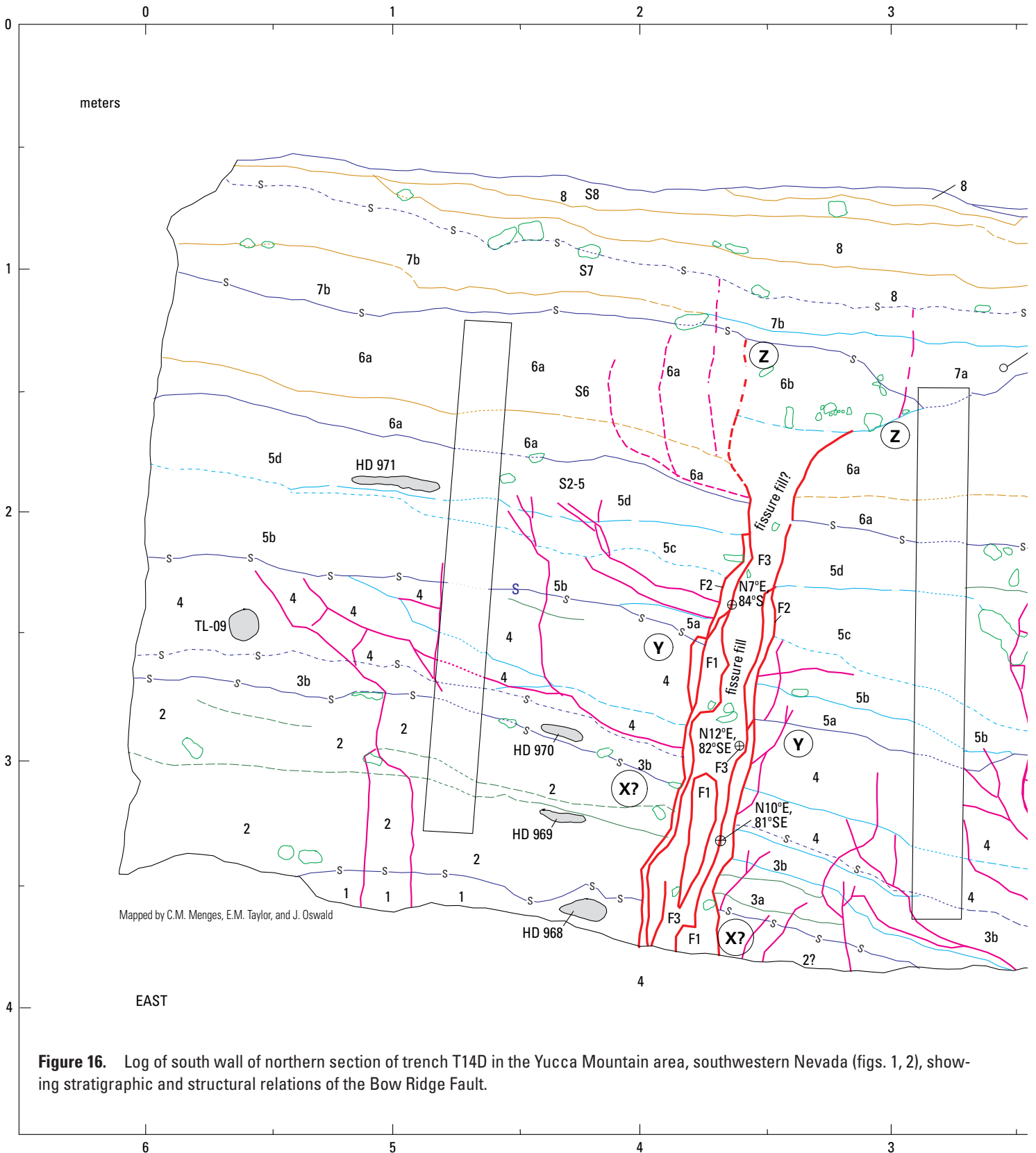
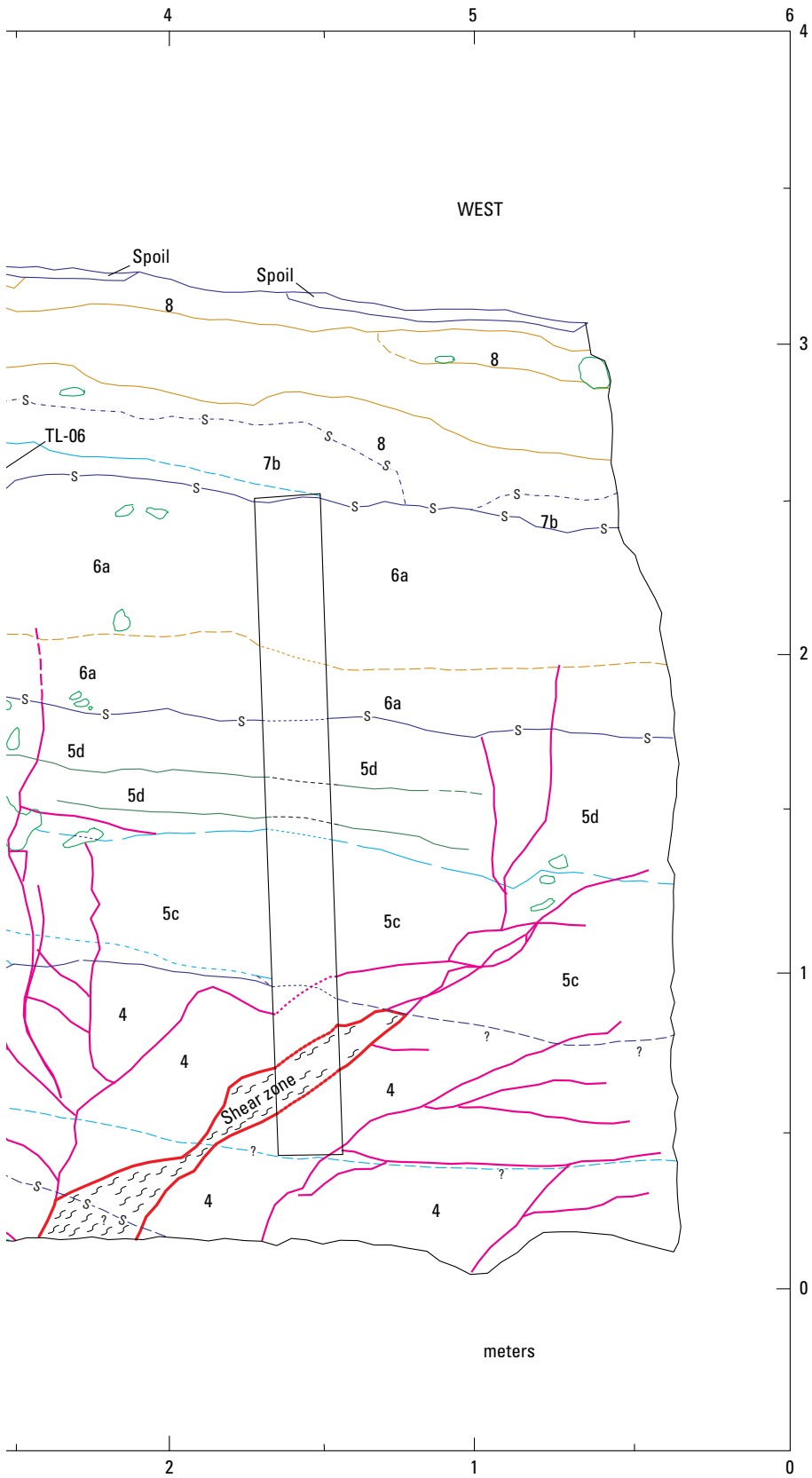


Figure 16. Log of south wall of northern section of trench T14D in the Yucca Mountain area, southwestern Nevada (figs. 1, 2), showing stratigraphic and structural relations of the Bow Ridge Fault.



EXPLANATION

- Lithologic-unit boundary**—Dashed where approximate, dotted where concealed, queried where uncertain
- Fault boundary**—Dashed where approximate, dotted where concealed, queried where uncertain
- Fractures and shears**—Dotted where concealed, queried where uncertain
- Free-face boundary**
- Lithologic-subunit boundary**—Dashed where approximate, dotted where concealed, queried where uncertain
- Combined lithologic-unit/soil-horizon boundary**—Dashed where approximate, dotted where concealed, queried where uncertain
- Soil-horizon boundary**—Dashed where approximate, dotted where concealed, queried where uncertain
- Carbonate laminae**—Dashed where approximate, dotted where concealed
- Paleosurface corresponding to a buried fault scarp**
- Single clasts or clustered gravel clasts**
- Sample locality for dated material**—Number refers to sample listed in table 9
- Lithologic unit**
- Faulting-event horizon**
- Shoring**
- Strike and dip directions**

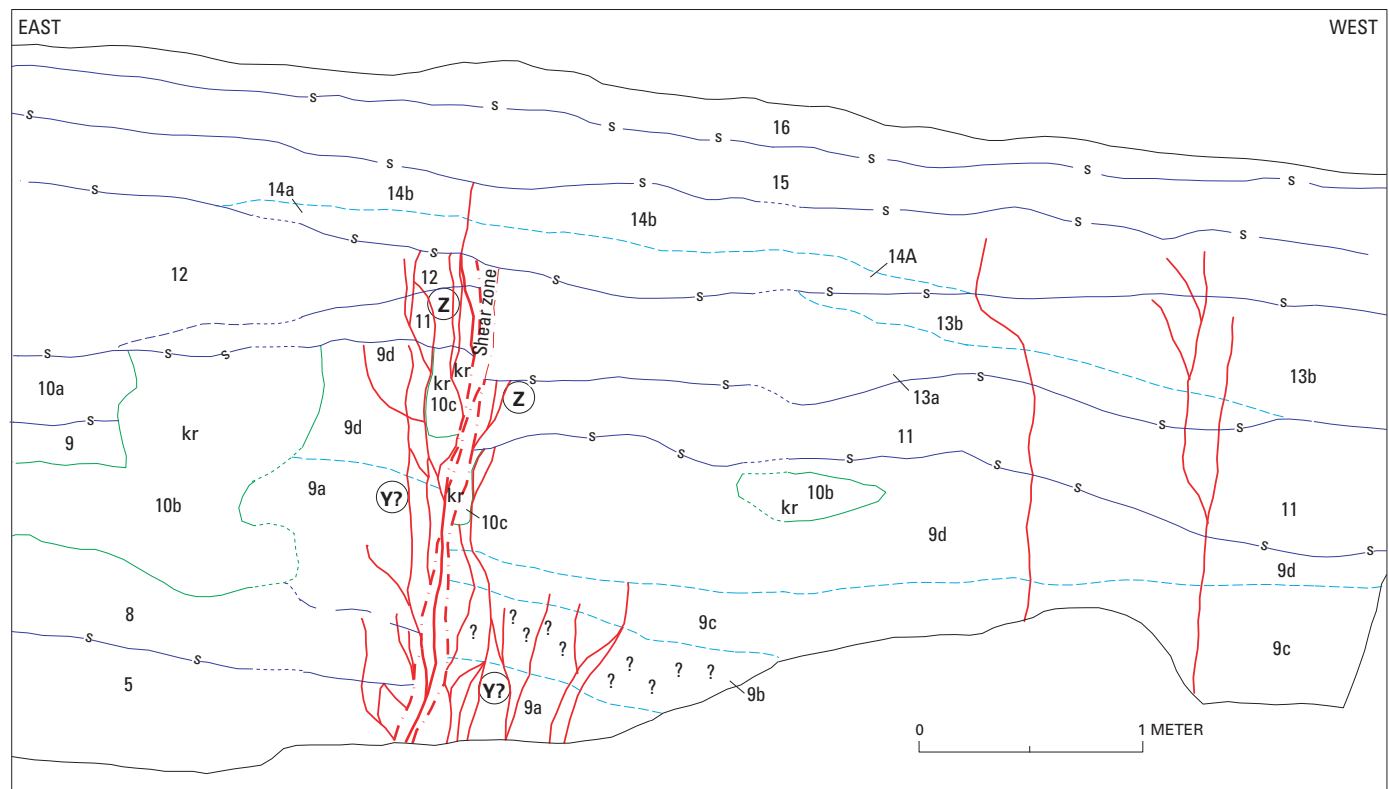
Orientation: N. 75° W.

gravel that appear to be more cemented by carbonate and silica with increasing age of faulting. Numerous aligned clasts were observed in both walls of the trench that reflect fissure infilling or buildup of colluvial wedges against scarp-free faces. The fault trace is terminated abruptly by undisturbed colluvial deposits exposed in the uppermost 1 m of the trench (units 7, 8, fig. 16; units 14, 15, fig. 17). The lowermost unfaulted units (unit 7, fig. 16; unit 14, pl. 3) are locally fractured, but not displaced, above the fault. Numerous small secondary fault strands and fractures with little to no offset are within 2 to 3 m of the main fault trace.

Two to three middle to late Pleistocene faulting events are evident in trench T14D (figs. 2, 16, 17; table 6). A possible early faulting event (X, table 8) near the bottom of the trench (northern section, fig. 16) is identified by an apparent increase in stratigraphic offset of unit 2 and by a possible colluvial wedge (unit 3a, fig. 9), although that event is difficult to identify with certainty because of poor stratigraphic definition and pedogenic overprinting. Two later events (Y, Z) are more clearly defined and are recognized on the basis of multiple criteria, including

(1) incremental upsection decrease in the offsets of successive marker horizons, (2) differential development of fissure fills and carbonate coatings that terminate at specific horizons, (3) local upward terminations of fractures at a given horizon, and (4) small colluvial wedges (units 5a, 7a, fig. 9) possibly related to scarp degradation after surface rupture. In the southern section of the trench (fig. 17), event Z is especially well defined by a conspicuous gravelly colluvial wedge, but evidence for penultimate event Y is more ambiguous in this exposure.

Dip-slip displacements per event range from 1 to 46 cm (preferred value, 12–40 cm; tables 7, 8). Cumulative displacements of unit 4 (fig. 9) in the northern section of the trench are small (30–45 cm); vector addition of the oblique-slip component increases the net cumulative displacement of this horizon to 33–70 cm. Similar adjustments also indicate net oblique-slip displacements per event ranging from 1 to 15 cm for smaller faulting events and from 46 to 80 cm for larger faulting events (preferred value, 13–44 cm). Fractures with no displacement were formed in unit 7 (northern section of trench, fig. 16) and unit 14 (southern section of trench, fig. 17) above the main fault



EXPLANATION

- | | |
|---|--|
| - - - Faults and fractures—Dashed where inferred | - - - Lithologic-subunit horizon |
| - · - · - Fissure-fill boundary | 13b Lithologic-unit number |
| - s - - - Lithologic-unit boundary—Dashed where inferred, dotted where inferred | Ⓨ? Faulting-event horizon—Queried where uncertain |
| - · - · - Combined lithologic-unit/soil-horizon boundary—Dotted where indistinct | Ⓚr Krotovina |

Figure 17. Log of south wall of southern section of trench T14D in the Yucca Mountain area, southwestern Nevada (figs. 1, 2), showing stratigraphic and structural relations of the main Bow Ridge Fault zone.

trace, although these features may be nontectonic in origin or related to ground motion on another fault. The size of individual and cumulative late Quaternary displacements at a given stratigraphic level decreases northward along the fault zone from trench T14D to trenches T14C and T14 (fig. 2).

The timing of faulting events was estimated by correlating trench units with the surficial deposits mapped in Midway Valley (tables 2, 4; Wesling and others, 1992), and numerically by U-series and thermoluminescence analyses of selected deposits in the northern section of trench T14D (figs. 2, 8, 16). The oldest faulted colluvial unit in the footwall block (unit 1, fig. 16) is early Pleistocene, on the basis of a U-series age of 700 ka on pedogenic carbonate (sample HD 968, fig. 16; table 9), although its downfaulted equivalent is not exposed on the hanging-wall block. Above this unit is a package of mixed middle to upper Pleistocene colluvial and eolian deposits. Poorly constrained U-series ages of $340 \pm \infty / -120$ and $234 \pm 47 / -35$ ka (samples HD 969 and HD 970, respectively, table 9) were obtained on two samples collected from laminae in a calcic soil developed on units 2 and 3 (fig. 16) that postdates the possible earliest faulting event (X) in the trench. A thermoluminescence age of 132 ± 23 ka (sample TL-09) was obtained from a mixed eolian-colluvial deposit (unit 4, fig. 16), the top of which forms the event horizon for the penultimate faulting event (Y). Carbonate laminae from a calcic soil developed in the overlying unit 5 that is cut by the most recent faulting event yielded a U-series age of 98–144 ka (sample HD 971). A close minimum date for the most recent surface-rupturing event is established by a thermoluminescence age of 48 ± 20 ka (sample TL-06) from unit 7a (fig. 16), which is interpreted as the fine-grained facies of the colluvial wedge deposited after the event. These timing constraints indicate general ranges of 130–30 and 150–130 ka for the dates of events Z and Y, respectively (table 10).

The available age control on faulting events indicates average recurrence intervals ranging from 75 to 215 k.y. (preferred value, 100–140 k.y.; table 11) and individual recurrence intervals ranging from 40 to 350 k.y. (preferred value, 90–210 k.y.). Fault-slip rates computed on unit 4 in the northern section of the trench and on unit 9d in the southern section range from 0.002 to 0.007 mm/yr (preferred value, 0.003 mm/yr; tables 11, 12). We note, however, that these slip rates are necessarily based on only two faulting events, with one intervening interval, and that the slip rates include the effect of the time elapsed since the most recent event, which somewhat limits their significance although no other paleoseismic data are presently available. Long recurrence intervals are supported by such features in the trench as petrocalcic soils developed on units deposited between faulting events and several buried, degraded fault scarps formed above colluvial wedges associated with event horizons.

Trench T14

As mentioned earlier, trench T14 (pl. 3; figs. 2, 8) provides little information for interpreting the history of Quaternary activity on the Bow Ridge Fault but does yield valuable data on the nature and origin of secondary carbonate and silica

veins that intersect both Quaternary deposits and Tertiary bedrock within the main fault zone. Bedrock is exposed at the east end of the trench, and Quaternary deposits at the west end; in between is a well-defined, 2.5- to 4-m-wide vertical fissure-filled fault zone (pl. 3).

During the course of trench-wall mapping, Taylor and Huckins (1995) distinguished 12 colluvial units within the Quaternary stratigraphic sequence on the north wall of trench 14 and 10 units on the south wall (pl. 3). Except for two units absent on the south wall, these deposits can be correlated across the trench. The colluvial units consist of poorly sorted, poorly bedded soft sand to silty sand and pebble-cobble gravel that becomes indurated where cemented by carbonate and opaline silica. The gravel content ranges from about 5 to as much as 80 volume percent with increasing trench depth. The dip of the colluvial depositional packages, defined by bedding and subparallel stringers and laminae of carbonate and opaline silica, flattens from 30°–60° SW. in the basal unit to 8°–10° SW. in the upper unit (pl. 3).

Although surficial deposits are in fault contact with brecciated volcanic tuff (pl. 3), no measurable displacements were observed within the Quaternary sequence from which to determine the magnitude and date of individual faulting events. The trench T14 exposure provides evidence, however, that before the depositional period represented by units 5S through 8S (south wall, pl. 3), two colluvial wedges that probably reflect two faulting events were deposited against fault scarps which were later beveled by erosion. Units 5S through 8S were reported by Taylor and Huckins (1995) to range in age from 270 ± 90 to 488 ± 90 ka, on the basis of U-trend dates (samples YM 14 10–14, YM 14 15–17, YM14 18–22, table 9). Sometime later, but before deposition of the upper K soil horizon that caps unit 8S (88 ± 5 ka; sample HD 1–A, table 9), two or more other fracturing or faulting events occurred. Subsequently, other fractures formed and were filled with black ash, whose source is considered to be from an eruption of the nearby Lathrop Wells volcanic center at 77 ± 6 ka (Heizler and others, 1999).

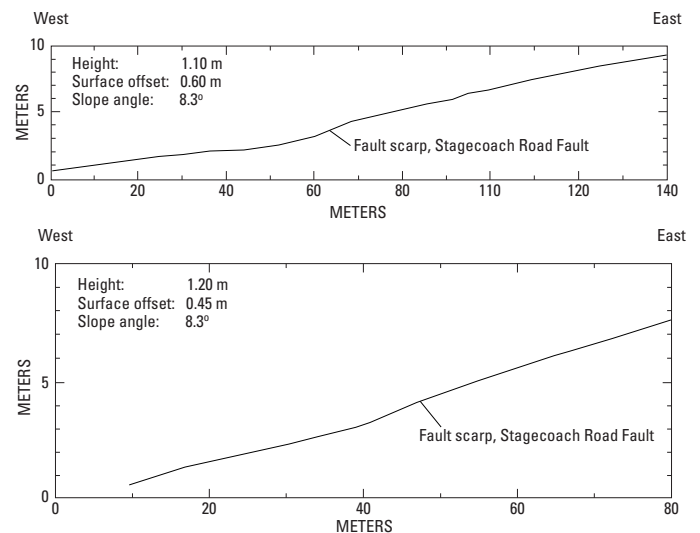
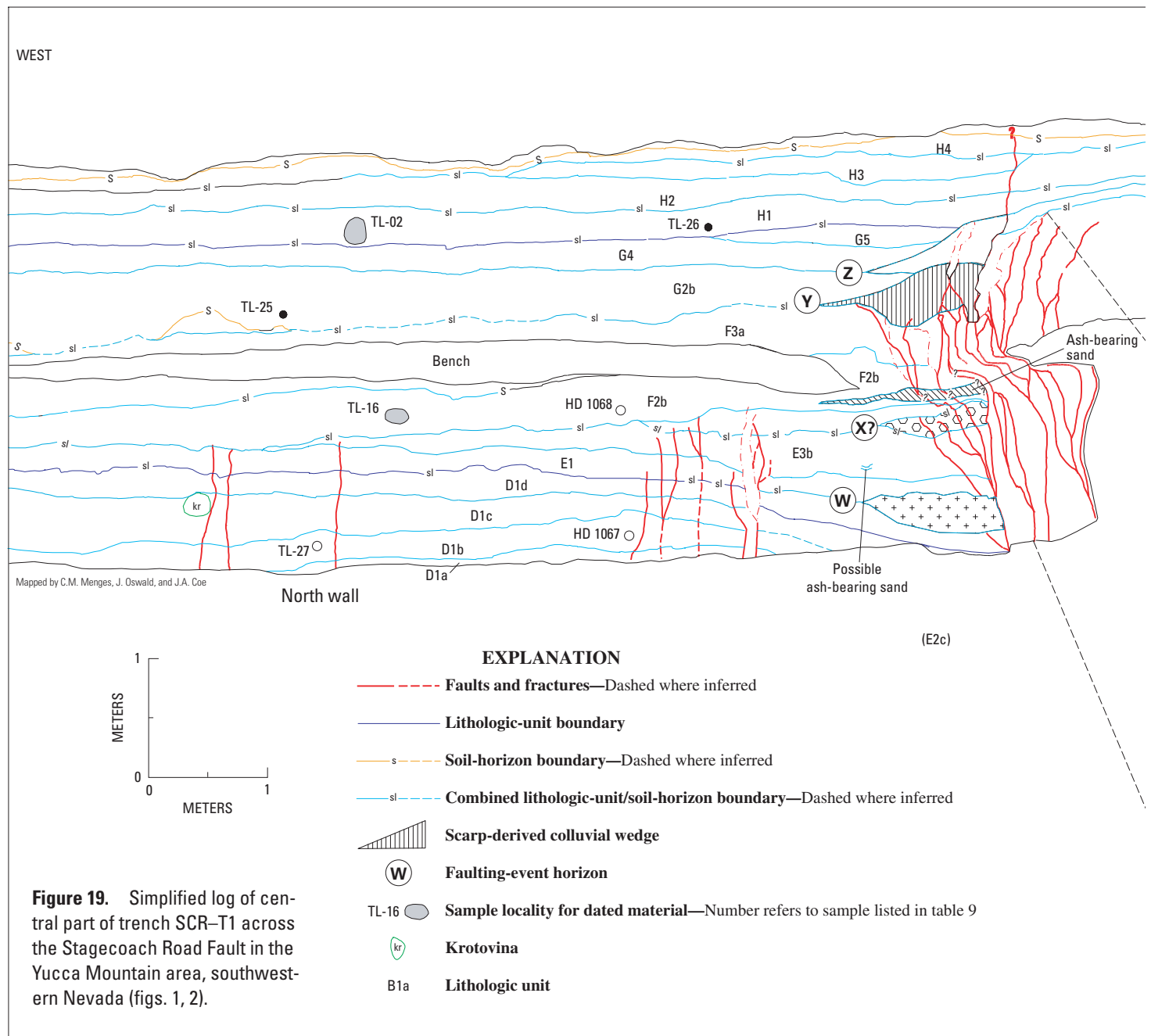


Figure 18. Topographic profiles of geomorphic surfaces across the Stagecoach Road Fault in the Yucca Mountain area, south-western Nevada (figs. 1, 2).

The fissure-filled Bow Ridge Fault zone in the central part of trench T14 (pl. 3) is characterized by vertical veins containing fine-grained sediment, secondary carbonate and opaline silica, and black ash (Taylor and Huckins, 1995), with a minor component (<5 volume percent) of local volcanic-rock fragments. The ash loosely fills some fractures, which generally are near the center of vertically oriented veins; locally, however, the ash-filled fractures are adjacent to the surrounding bedrock. Laminae of secondary carbonate and silica range in thickness from 0.2 to 10 cm but are not continuous for more than 20 to 30 cm.

The origin of the secondary carbonate- and silica-filled veins—whether by ascending or descending water—has been

a matter of considerable controversy. Physical, chemical, mineralogic, biologic, petrographic, and isotopic data collected in trench T14 indicate that the vein fillings are characteristic of an environment with descending meteoric water—that is, a pedogenic environment. Supporting evidence, such as (1) lateral persistence of the colluvial deposits, (2) decrease in the concentration of secondary carbonate below a zone of maximum concentration, (3) presence of discrete soil horizons, and (4) isotopic ratios consistent with those of meteoric water, was discussed in detail by Taylor and Huckins (1995). In summary, the interpretation is that episodes of faulting temporarily created open fractures that formed conduits for percolating water and for the accumulation of fine-grained materials.



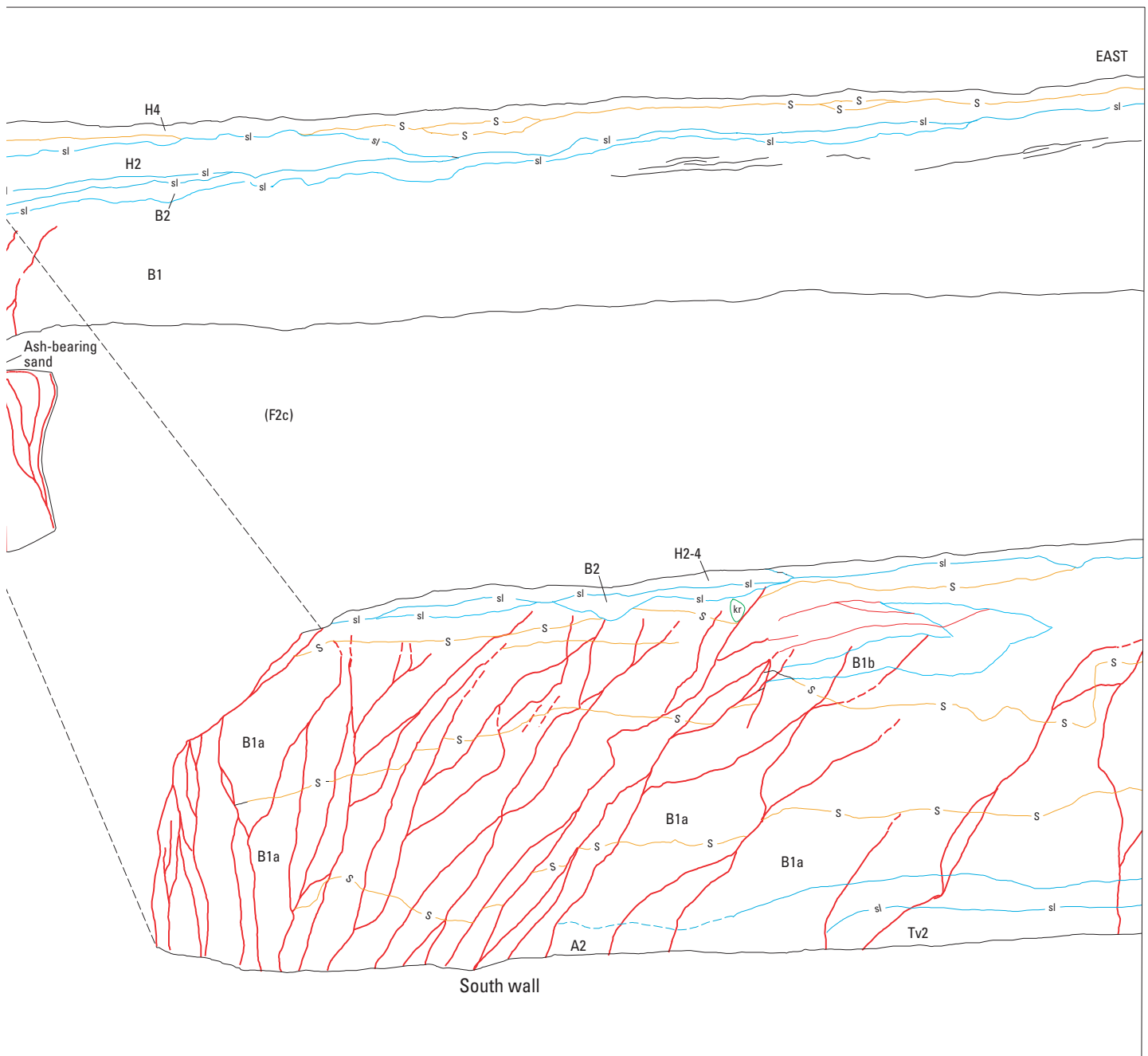
Movement of water within the fractures was enhanced after the deposits were cemented by carbonate and opaline silica and subsequently fractured. Surface runoff percolated through the near-vertical fractures and precipitated carbonate laminae.

Stagecoach Road Fault

Trenches SCR-T1 and SCR-T3

The Stagecoach Road fault (figs. 2, 4), though recognized as a potentially important Quaternary fault (O'Neill and others, 1991), was not evaluated by paleoseismic studies

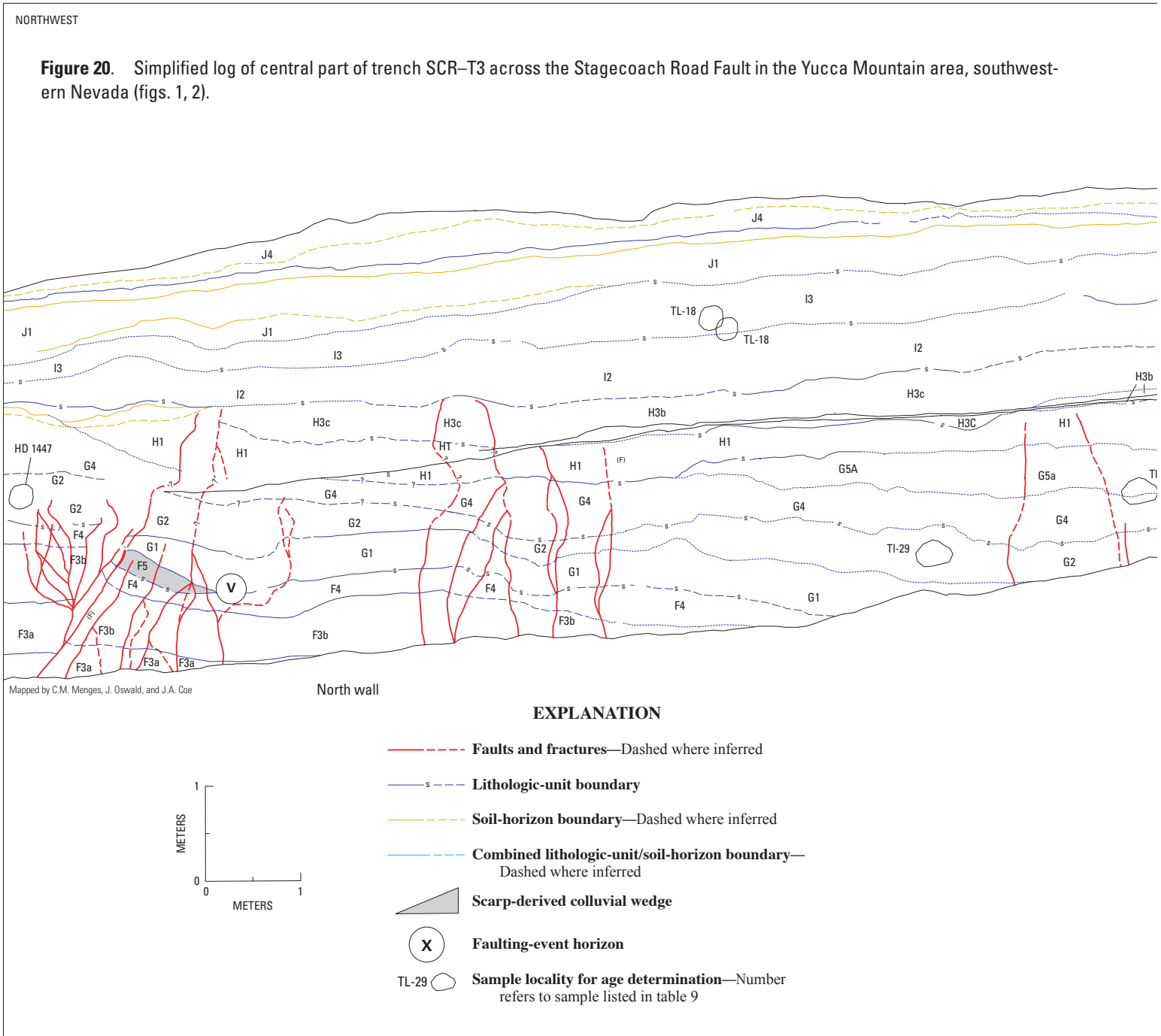
until three trenches, SCR-T1 through SCR-T3 (fig. 2), were excavated across it in September 1992. The main fault trace is defined by a distinct scarp. At two trench sites, the scarp is 1.1 to 1.3 m high and has a maximum slope of 8° (fig. 18). Two of these trenches (SCR-T1, SCR-T3), which are located within 2 km of each other on the main fault trace (fig. 2), exhibit fundamentally similar structural and stratigraphic relations; these trenches are discussed together herein, and both were described in greater detail in Menges and others (1998). A third trench (SCR-T2) was excavated across the projection of a bedrock fault south of trench SCR-T1 but was not logged (and is not discussed further here) because no Quaternary deformation was observed at the site.



Trenching studies were augmented by drilling three shallow boreholes in August 1994 near trench SCR-T1. Two adjacent boreholes (SR-1, SR-2) with offset, but partly overlapping, depth ranges were drilled 50 m west of the fault zone that is exposed in the trench; a third borehole (SR-3) is located 75 m west of the fault. The drill holes were designed to sample units at depth within the hanging-wall block. Specific objectives included determination of depth to bedrock and a search for carbonate soils in the hanging-wall block comparable in strength of development to the petrocalcic soils in the footwall block (see below).

The fault as exposed in trenches SCR-T1 and SCR-T3 juxtaposes markedly different stratigraphic and soil sequences of mixed alluvium, colluvium, and eolian material on the hanging-wall and footwall blocks (figs. 19, 20). The footwall blocks contain a 2- to 3-m-thick sand-and-gravel layer deposited across the west-sloping erosional surface cut across Tertiary volcanic bedrock. A distinctive reworked volcanic tuff is exposed at the base of surficial deposits in the footwall block of trench SCR-T1 (unit Tv2, fig. 19). The hanging-wall blocks lack deposits correlative with footwall-block units and instead contain younger sequences of locally gravelly alluvium, mostly unconsolidated

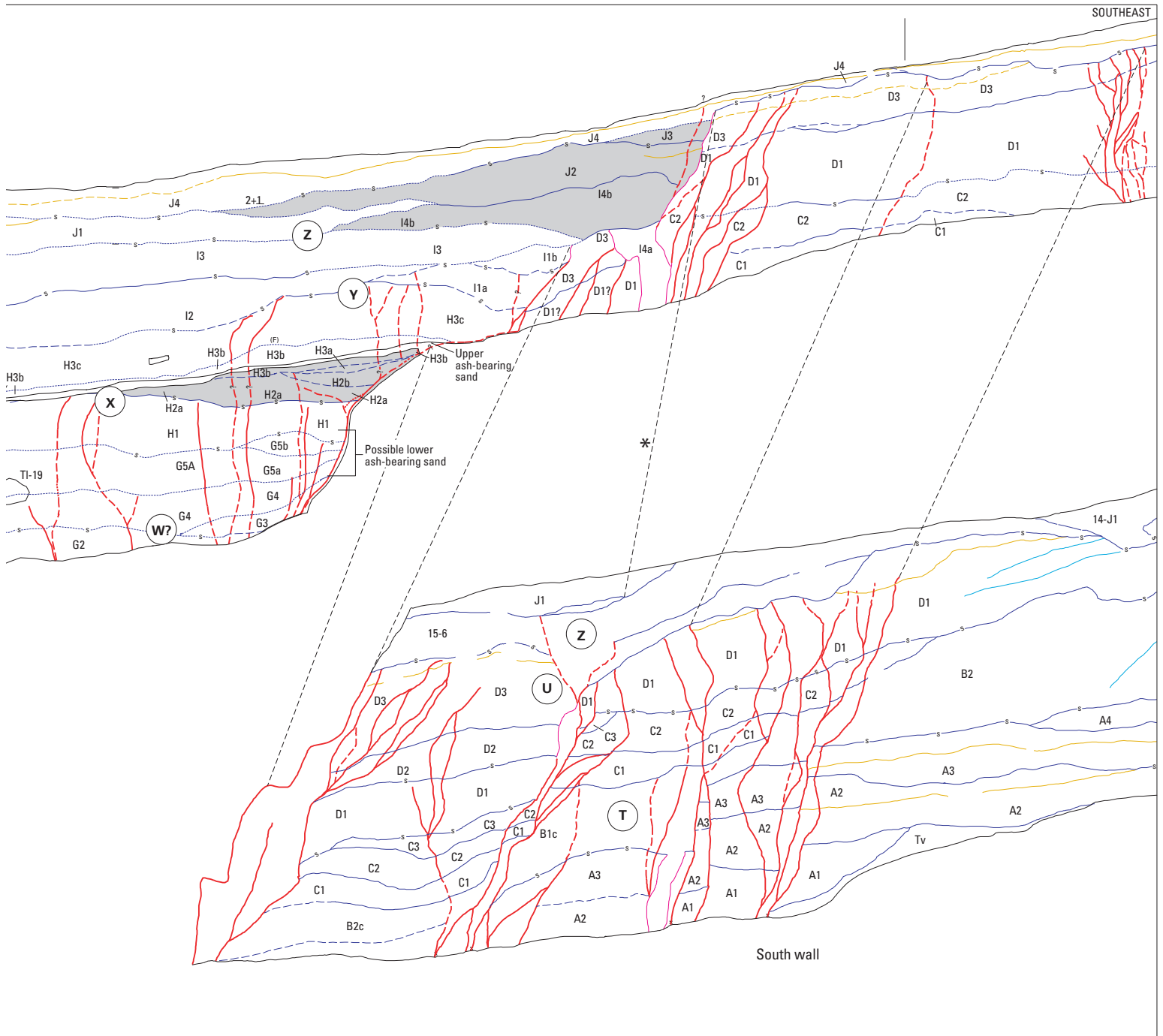
Figure 20. Simplified log of central part of trench SCR-T3 across the Stagecoach Road Fault in the Yucca Mountain area, southwestern Nevada (figs. 1, 2).



sandy colluvium and eolian material (sequences D–H, fig. 19; sequences G–J, fig. 20). These deposits typically consist of fine-grained sand and silt that are poorly bedded to massive and thus lack sharp stratigraphic definition. One or two thin undeformed sand and silt layers (units H1–H2, fig. 19; unit J4, fig. 20) continue along the entire length of the trenches and bury the fault zone. A strong contrast in the degree of soil development was observed across the fault as well. Well-developed carbonate-cemented (CaCO_3 stage III–V morphology) petrocalcic soils have formed at the upper surface of the footwall blocks in both trenches, whereas soils on the hanging-wall blocks typically are

weakly to only moderately well developed. The maximum carbonate development observed in any of the soils exposed in the middle and upper parts of trench walls generally does not exceed CaCO_3 stage I–II+ morphology and cambic B horizon.

The boreholes west of trench SCR–T1 penetrated 82 to 101 m of unconsolidated to poorly consolidated fine-grained deposits, consisting mostly of sand and silt with local gravel layers that were deposited above weathered bedrock. These deposits contain numerous zones of dispersed carbonate but lack thick well-developed petrocalcic soils. A tuffaceous sand layer at 99-m depth that overlies a welded tuff in borehole



SR-3 is correlated with a similar pumiceous tuff (unit Tv2, fig. 19) in the footwall block of trench SCR-T1.

The Stagecoach Road Fault is well expressed in both trenches as multiple-strand zones containing numerous carbonate-coated shears and fractures (figs. 19, 20). The fault zone in trench SCR-T3 consists of four discrete, closely spaced strands, and another fault strand is present 20 m to the east of the main fault zone in the footwall block of trench SCR-T1 (located beyond section of trench shown in fig. 19). The dominant strike and dip of the fault zone is N. 0°–10° W., 85° W., in trench SCR-T1, where the fault trace deflects to the north, and N. 20°–30° E., 55°–65° W., in trench SCR-T3. The petrocalcic soil in the footwall block is extensively fractured adjacent to the main fault zone in trench SCR-T1 (fig. 19). The eastern fault strand is capped by this soil, and so deformation on that strand predates petrocalcic-soil development. The footwall block in trench SCR-T3 is undeformed east of the complex main fault zone (fig. 20). The hanging wall in both trenches is complexly deformed by secondary synthetic and antithetic fractures and shears that commonly are associated with eastward backtilting of strata toward the fault and by asymmetric graben formation adjacent to the main fault zone (figs. 19, 20). Previous surface mapping found evidence for significant amounts of left-oblique slip on the Stagecoach Road Fault (O'Neill and others, 1992); however, essentially dip slip slickenlines were observed on a bedrock fault strand that displaces overlying Quaternary deposits in the bottom of trench SCR-T3.

At least two, possibly as many as four, late Pleistocene to Holocene(?) faulting events were interpreted from deposits and structural relations observed on the hanging-wall block adjacent to the main fault zone in trench SCR-T1 (table 6), on the basis of such criteria as incremental downsection increases in stratal backtilting against the fault, upward termination of fractures and shears at discrete horizons, and the presence of colluvial wedges and fissures on the hanging-wall block. The wedges commonly are indistinct and lack stratigraphic definition.

The two latest faulting events (Y, Z, table 8) are represented by the best-defined surface ruptures in both trenches. The most recent event (Z) is interpreted from relations observed in the upper sedimentary sequence (unit G, fig. 19; unit I, fig. 20), such as fault truncations, displaced wedges from the penultimate event, and scarp-derived colluvial wedges. The penultimate event (Y), which is recognized at the top of the uppermost calcic soil (in unit F3a, fig. 19, and unit H3c, fig. 20), is associated with several fracture terminations, colluvial wedges, and fissures. A single fracture with no detectable offset was formed in otherwise undisturbed deposits (units H1–H4, fig. 19; unit J4, fig. 20) that bury the fault trace in each trench. These fractures may be either nontectonic in origin or related to ground shaking from a nearby paleoearthquake; thus, they are not necessarily associated with a surface-rupturing paleoearthquake on the Stagecoach Road Fault.

Faulting events are more difficult to identify in the poorly stratified and structurally overprinted deposits in the

lower parts of the trench walls, although the presence of progressively backtilted units downfaulted against footwall sequences requires additional faulting events within that interval. One faulting event (X) is inferred at the top of unit E3b in trench SCR-T1 (fig. 19) and above unit H1 in trench SCR-T3 (fig. 20), on the basis of upward fracture truncations, stratal backtilting, and indistinct colluvial wedges. Similar criteria were used to define a possible fourth faulting event (W) near the base of the exposures in the hanging-wall blocks in both trenches.

The three latest faulting events (X–Z) can easily be correlated between trenches. An earlier event (W) that also is correlated, on the basis of similarities in stratigraphic relations between the trenches, might be a discrete event in each trench. In trench SCR-T3, an earlier faulting event (V) is identified on the antithetic bounding fault of the hanging-wall graben, although the affected tilted deposits project eastward beneath the trench bottom before reaching the main fault trace. Two additional earlier faulting events (T, U) are present only on eastern strands of the fault on the footwall block in trench SCR-T3.

Displacements are difficult to estimate because of the absence of most hanging-wall units on the footwall block. Apparent dip slip was estimated from the thicknesses of colluvial wedges, which are considered minimums, and from the total stratigraphic thicknesses between event horizons, which represent maximums. Displacements per event range from 15 to 160 cm, commonly from 40 to 100 cm (tables 7, 8). Cumulative displacements near the bottoms of trenches range from 117 to 493 cm; corrections for local backtilting of units and graben formation reduce the amount of net slip to 28–79 cm for individual events and to 99–309 cm for net cumulative offsets.

No direct age determinations are available for units in the footwall block in either trench. Footwall deposits are approximately dated at middle Pleistocene in trench SCR-T3, on the basis of soil development. The thick, well-developed petrocalcic soil in trench SCR-T1 indicates an age of at least early Pleistocene, possibly Pliocene, for surficial units above bedrock in the footwall block.

Various geochronologic data—including both U-series and thermoluminescence analyses and the correlated age of basaltic ash disseminated within sandy layers—establishes a late Pleistocene through Holocene age for the hanging-wall deposits in both trenches (figs. 19, 20; tables 6, 7, 9). Some of the U-series and thermoluminescence ages summarized herein differ slightly from those of Menges and others (1998), and the age assignment and significance of the ash-bearing strata have also been adjusted from their report. Rhizolith-rich sandy layers containing evidence for one or two poorly defined faulting events (W, X) are exposed in the lower half of trench SCR-T1 (fig. 19). These rhizoliths yielded U-series ages ranging from 13±6 to 27±1 ka (samples HD 1068 and HD 1067, respectively, table 9) that are considered minimum ages because the dated carbonate in rhizoliths replaces plant roots that postdate deposition of the unit by an unknown, but

potentially significant, time interval. Older depositional ages for this stratigraphic interval are indicated by thermoluminescence ages of 28 ± 4 and 49 ± 9 ka (samples TL-16, TL-27) from units F2b and D1b, respectively, in trench SCR-T1 (fig. 19); however, a lithologically similar stratigraphic interval in the lower part of trench SCR-T3 (fig. 20) may be even older, on the basis of a thermoluminescence age of 87 ± 18 ka (sample TL-19) from unit G5 and U-series ages from an underlying carbonate soil in unit G2 of about 80–115 ka (sample HD 1447)—significantly older than a thermoluminescence age of 60 ± 16 ka (sample TL-29), also from unit G2. Thus, similar stratigraphic intervals in the lower parts of both trenches have two sets of only slightly overlapping U-series or thermoluminescence estimated ages: one set approximately 30–60 ka and the other set closer to 80–110 ka. The older ages are preferred for the lower section containing events W(?) and X in both trenches because (1) they provide the best concordance between both geochronologic methods in trench SCR-T3 and (2) the older ages agree better with the stratigraphic positions and correlated ages of basaltic ash observed in both trenches, as described below. The older age is also more consistent with the degree of soil development associated with unit G2 in trench SCR-T3.

Disseminated but distinctive basaltic ash is present in a sandy layer at approximately the same stratigraphic position in both trenches (units F2c and H3c in trenches SCR-T1 and SCR-T3, respectively, figs. 19, 20). Preliminary geochemical analysis of the ash from trench SCR-T1 indicates a source from the nearby Lathrop Wells volcanic center (F.V. Perry, written commun., 1996), which erupted at 77 ± 6 ka (Heizler and others, 1999). That age is consistent with the position of the ash-bearing layer relative to the older U-series and thermoluminescence ages (80–115 ka) determined for the lower part of trench SCR-T3 described above, but it mostly lies outside the 30–60-ka interval indicated by the oldest thermoluminescence age in that trench and both of the older thermoluminescence ages in trench SCR-T1.

A second ash-bearing horizon was identified in each trench below the primary upper ash layer, but the stratigraphic context of these lower ash horizons is more problematic. The lower ash in trench SCR-T1 (figs. 2, 19) is concentrated in a small pocket within a sandy layer and so may represent an ash-filled krotovina (animal burrow) related to the overlying upper ash layer, whereas basaltic ash is extremely diffuse and dispersed in a poorly defined lower horizon in trench SCR-T3 (figs. 2, 20). The two ash horizons were originally considered by Menges and others (1998) to reflect multiple eruptions

at Lathrop Wells—the prevailing interpretation during early stages of the paleoseismic investigations at Yucca Mountain (Crowe and others, 1995; Menges and others, 1998). On the basis of the single eruption (77 ± 6 ka) reported by Heizler and others (1999), however, the present interpretation is that the upper ash-bearing horizon, which is well defined in both trenches, correlates with that eruption.

The slightly oxidized sand layer in the upper part of the hanging-wall block that overlies the penultimate-event Y horizon in trench SCR-T1 (unit G2b, fig. 19) yielded a thermoluminescence age of 12 ± 1 ka (sample TL-25, table 9); the thermoluminescence age of a lithologically similar unit in trench SCR-T3 with a similar stratigraphic relation to event Y is 22 ± 5 ka (units I2, I3, fig. 20; sample TL-18, table 9). Evidence for the most recent event (Z) in trench SCR-T1 is above faulted unit G2b, but is buried by an undeformed unit (unit H1, fig. 19) with two thermoluminescence ages of 12 ± 6 and 9 ± 1 ka (samples TL-02 and TL-26, respectively, table 9) that are consistent with the morphology of the soil developed on the colluvium, which is weakly developed with minimal secondary carbonate, similar to soils on uppermost Pleistocene to middle Holocene deposits in the Yucca Mountain area (figs. 1, 2).

Estimated recurrence intervals and slip rates vary, depending on which set of discordant ages is assigned to the stratigraphic units in the middle and lower sections of the trenches. The age assignment of 70–100 ka for that interval, based primarily on the ash correlations in both trenches and the older set of U-series and thermoluminescence ages in trench SCR-T3 (fig. 20), yields preferred average recurrence intervals of 20–50 k.y. and preferred individual recurrence intervals of 5–50 k.y. (table 11). A preferred slip rate of 0.02 to 0.03 mm/yr is consistently calculated in both trenches from several different datums, using both ash correlations and directly dated layers as independent age control (tables 11, 12). Preferred estimated average and individual recurrence intervals are shorter (10–30 and 5–30 k.y., respectively) and slip rates are higher (0.03–0.05 mm/yr) if the younger set of thermoluminescence ages in trench SCR-T1 are used to assign an age range of 30–60 ka for the middle to lower stratigraphic interval in the trench. As noted above, we prefer the older age assignment and resulting recurrence intervals and slip rates because of the better internal concordance among various geochronologic methods, including ash correlations. We consider the younger set of thermoluminescence ages in the lower part of the trenches to be unreliable, possibly contaminated by postdepositional infiltration and accumulation of younger eolian fines in these highly unconsolidated deposits.

